The Abdus Salam
International Centre for Theoretical Physics

United Nations
Educational, Scientific and
Cultural Organization

IAEA
International Atomic Energy Agency

2245-7

Joint ICTP-IAEA Advanced School on the Role of Nuclear Technology in Hydrogen-Based Energy Systems

13 - 18 June 2011

Neutron diffraction studies of metal hydrides
(Part 1)

J. Huot
Universite du Quebec a Trois-Rivieres
Canada
&
Institute for Energy Technology
Norway

The Abdus Salam
International Centre for Theoretical Physics

IAEA.org
International Atomic Energy Agency

Neutron diffraction studies of metal hydrides

J. Huot

Université du Québec à Trois-Rivières

UQTR
Université du Québec
à Trois-Rivières

Present address: *Institute for Energy Technology, Norway*

IFE Institute for Energy Technology

Joint ICTP-IAEA Advanced School on the Role of Nuclear Technology in Hydrogen-Based Energy Systems
Trieste – Italy, 13 – 18 June 2011

Content

1. AB_5 alloys.
2. BCC alloys
3. Complex hydrides
4. Magnesium

$LaNi_5$

- *Classic* metal hydride
- Low capacity (≈1.4 wt.%)
- Room temperature hydride
- Substitution of Ni by other transition metals could change the plateau pressure and resistance to cycling.
- Could also be used in electrochemistry

UQTR
Université du Québec
à Trois-Rivières

$LaNi_5$ structure

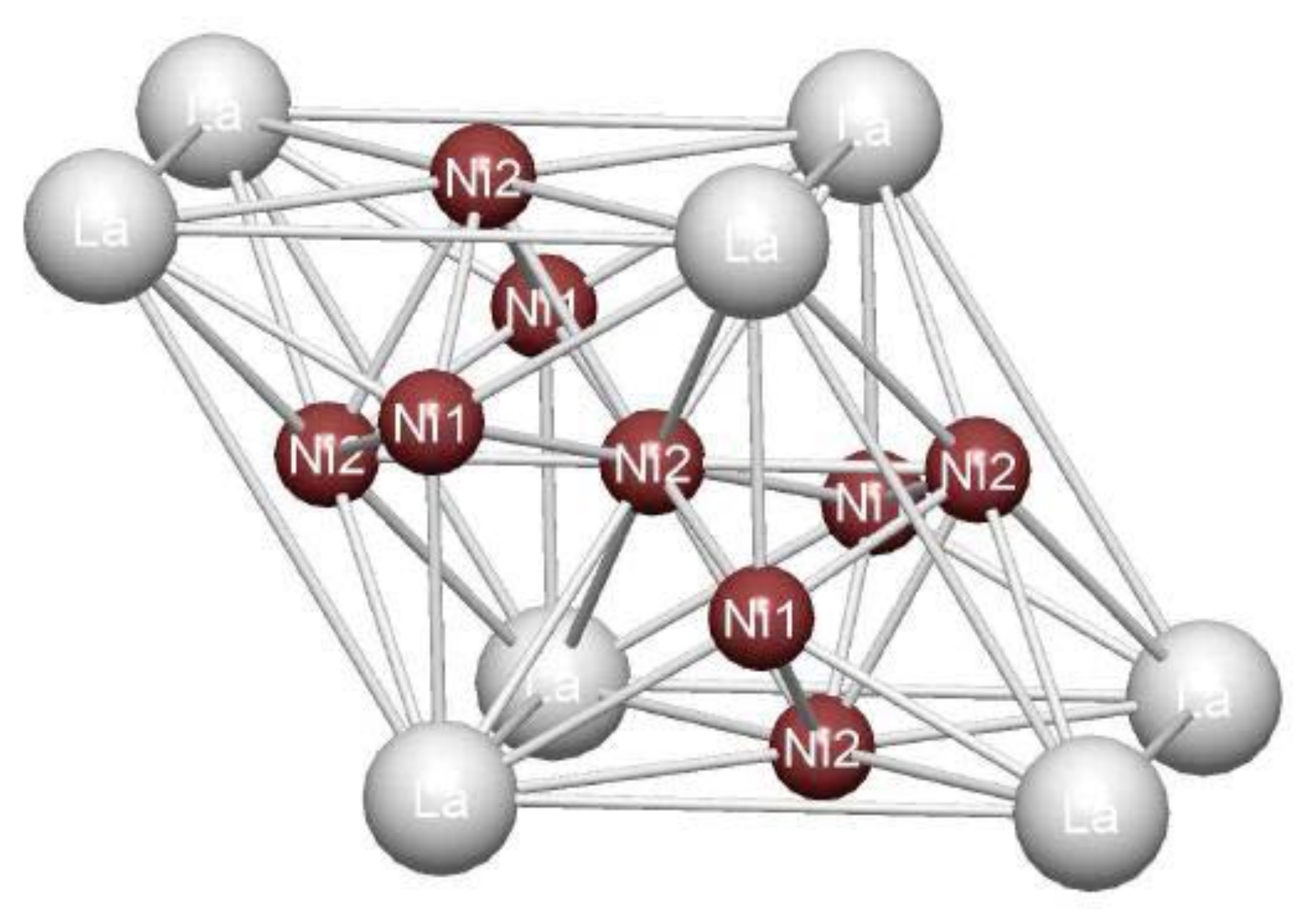

hP6, P6/mmm

$LaNi_5H_6$ structure

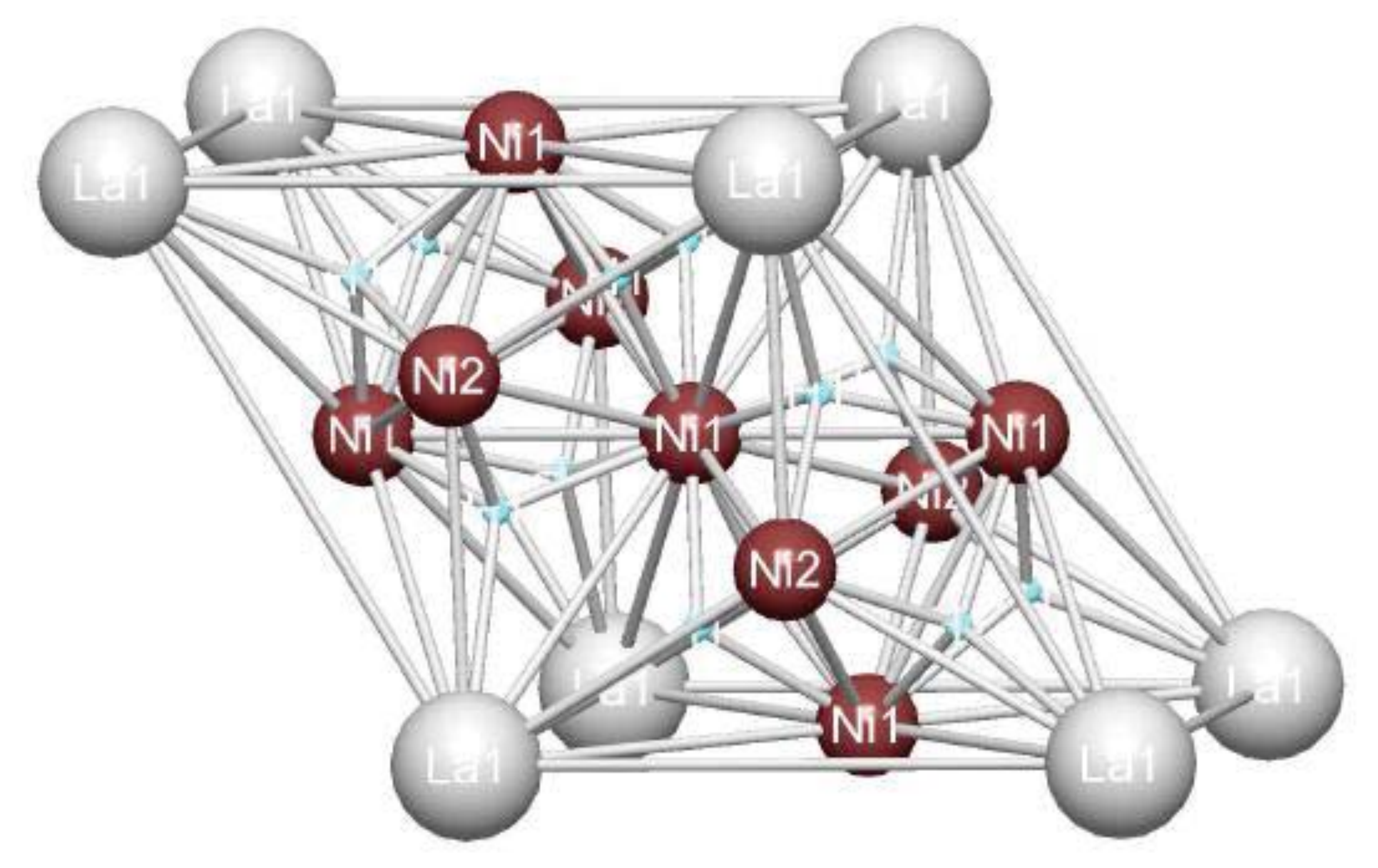

hP18, P6/mmm

UQTR
Université du Québec
à Trois-Rivières

LaNi$_5$ X-ray pattern

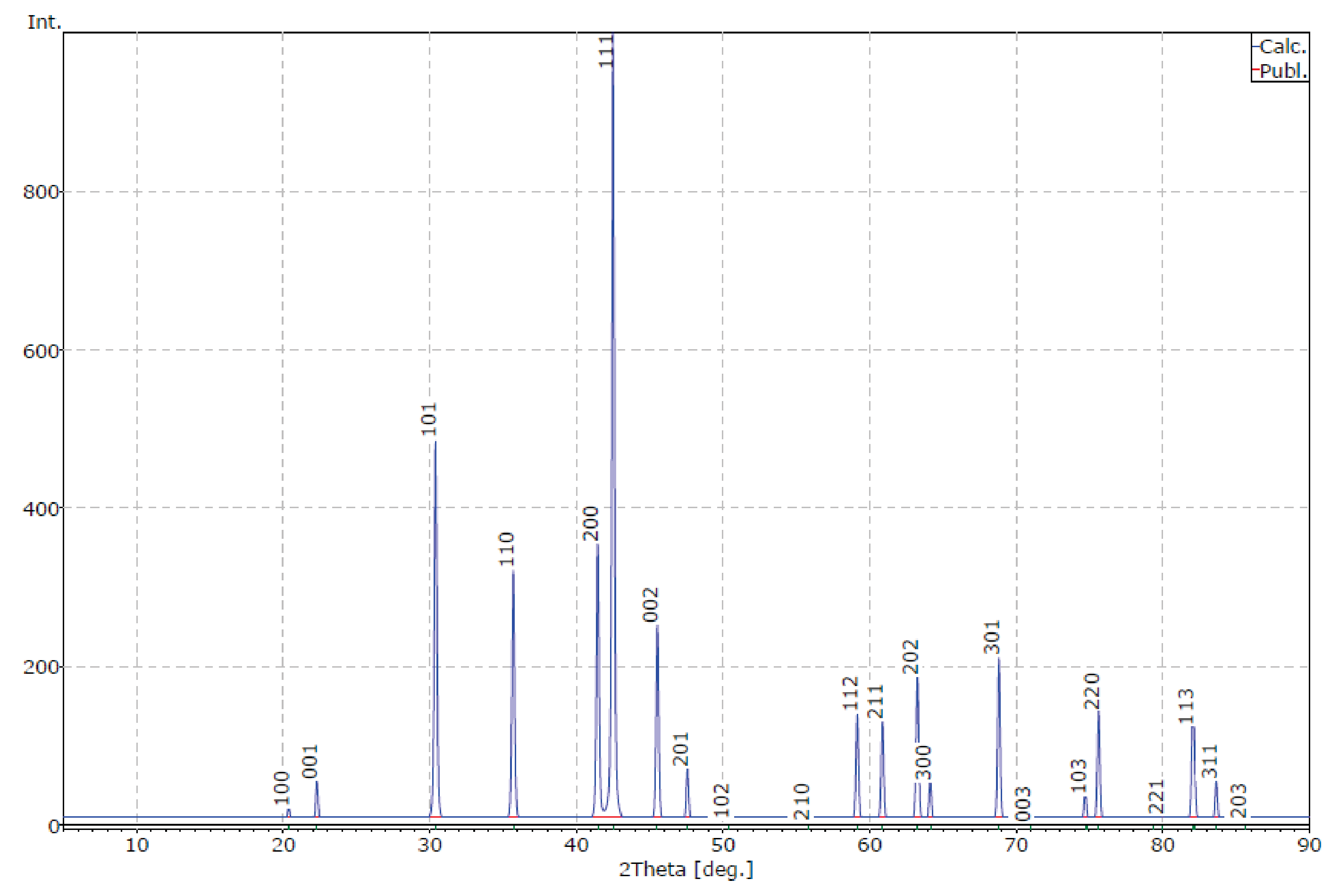

hP6, P6/mmm

UQTR
Université du Québec
à Trois-Rivières

$LaNi_5H_6$ X-ray pattern

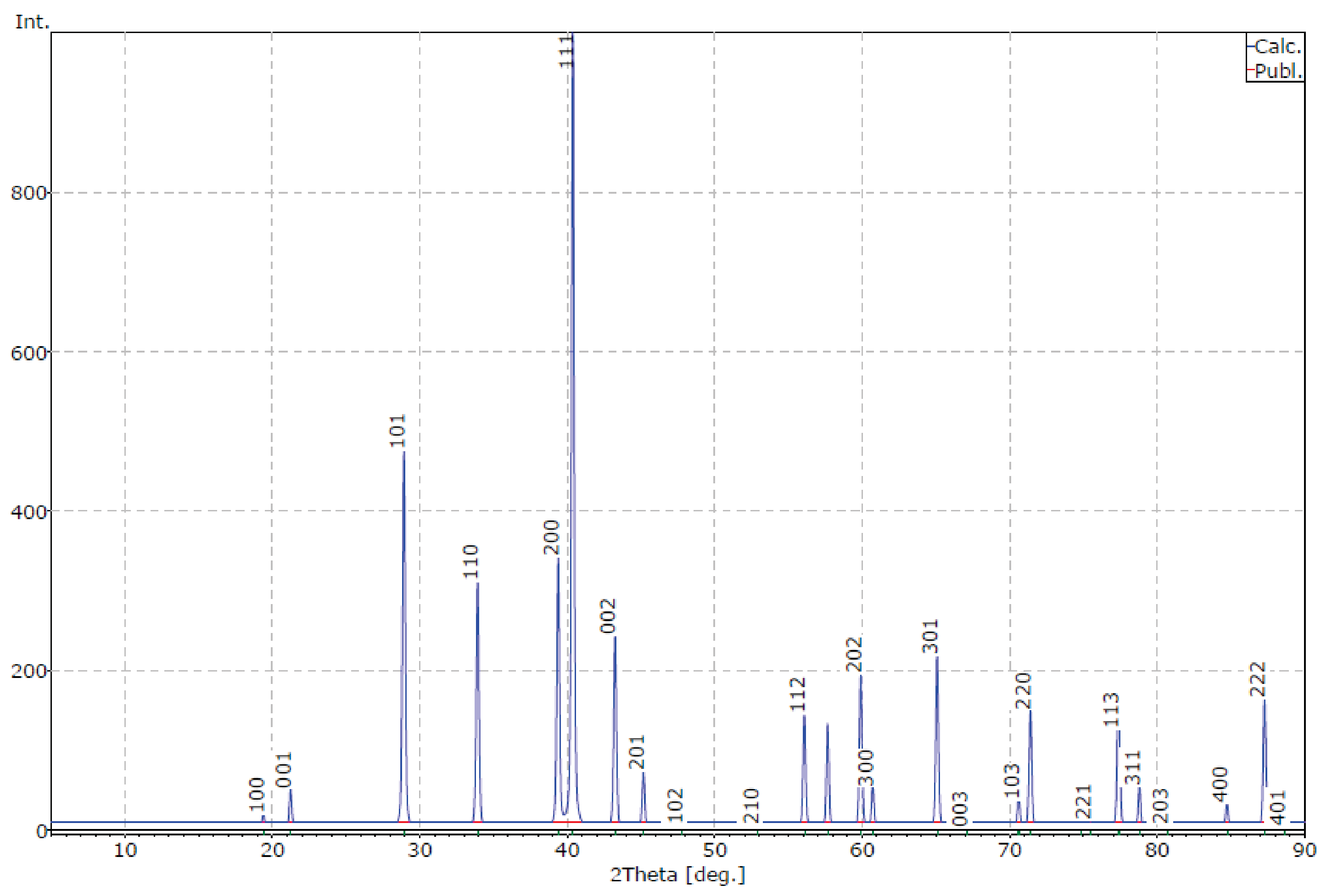

hP18, P6/mmm

Université du Québec
à Trois-Rivières

$LaNi_5$

- Metal and hydride phases have the same structure
- Hydrogen only occupy ½ of the sites
- Needs neutron to determine the exact location of hydrogen

$LaNi_5$

In-situ neutron diffraction during cycling allows bulk analysis of the material under geometry and conditions comparables to those of commercial batteries.

Possible to follow dynamically the structural response of the electrode as a function of charge and discharge rates

With high neutron flux high-rate capabilities of electrodes could be studied

UQTR
Université du Québec
à Trois-Rivières

$LaNi_5$

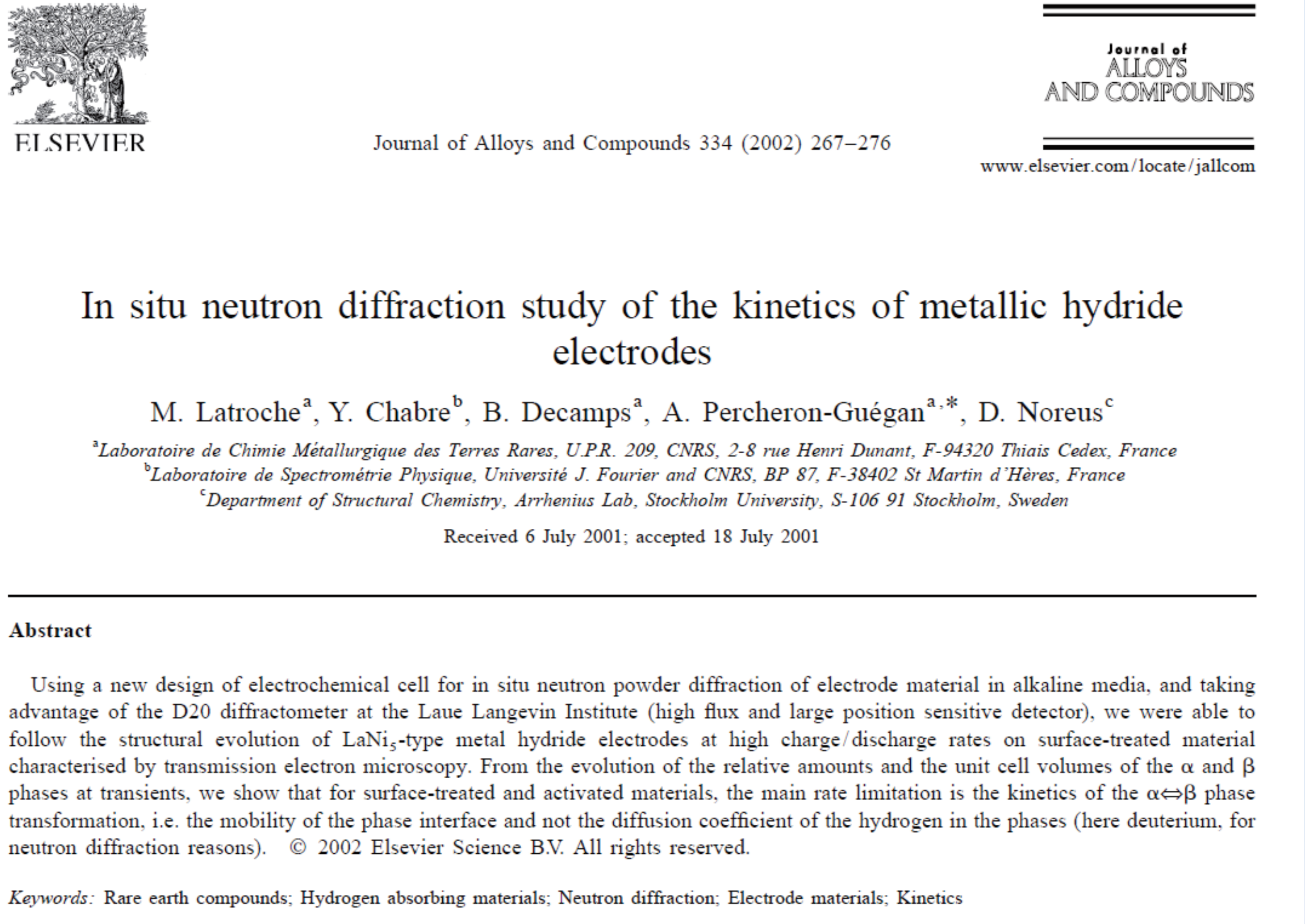

ELSEVIER

Journal of Alloys and Compounds 334 (2002) 267–276

Journal of ALLOYS AND COMPOUNDS

www.elsevier.com/locate/jallcom

In situ neutron diffraction study of the kinetics of metallic hydride electrodes

M. Latroche[a], Y. Chabre[b], B. Decamps[a], A. Percheron-Guégan[a,*], D. Noreus[c]

[a] *Laboratoire de Chimie Métallurgique des Terres Rares, U.P.R. 209, CNRS, 2-8 rue Henri Dunant, F-94320 Thiais Cedex, France*
[b] *Laboratoire de Spectrométrie Physique, Université J. Fourier and CNRS, BP 87, F-38402 St Martin d'Hères, France*
[c] *Department of Structural Chemistry, Arrhenius Lab, Stockholm University, S-106 91 Stockholm, Sweden*

Received 6 July 2001; accepted 18 July 2001

Abstract

Using a new design of electrochemical cell for in situ neutron powder diffraction of electrode material in alkaline media, and taking advantage of the D20 diffractometer at the Laue Langevin Institute (high flux and large position sensitive detector), we were able to follow the structural evolution of $LaNi_5$-type metal hydride electrodes at high charge/discharge rates on surface-treated material characterised by transmission electron microscopy. From the evolution of the relative amounts and the unit cell volumes of the α and β phases at transients, we show that for surface-treated and activated materials, the main rate limitation is the kinetics of the $\alpha \Leftrightarrow \beta$ phase transformation, i.e. the mobility of the phase interface and not the diffusion coefficient of the hydrogen in the phases (here deuterium, for neutron diffraction reasons).

Keywords: Rare earth compounds; Hydrogen absorbing materials; Neutron diffraction; Electrode materials; Kinetics

Studied the relative contributions of diffusion and phase transformations on the kinetic of bulk material

In-situ cell

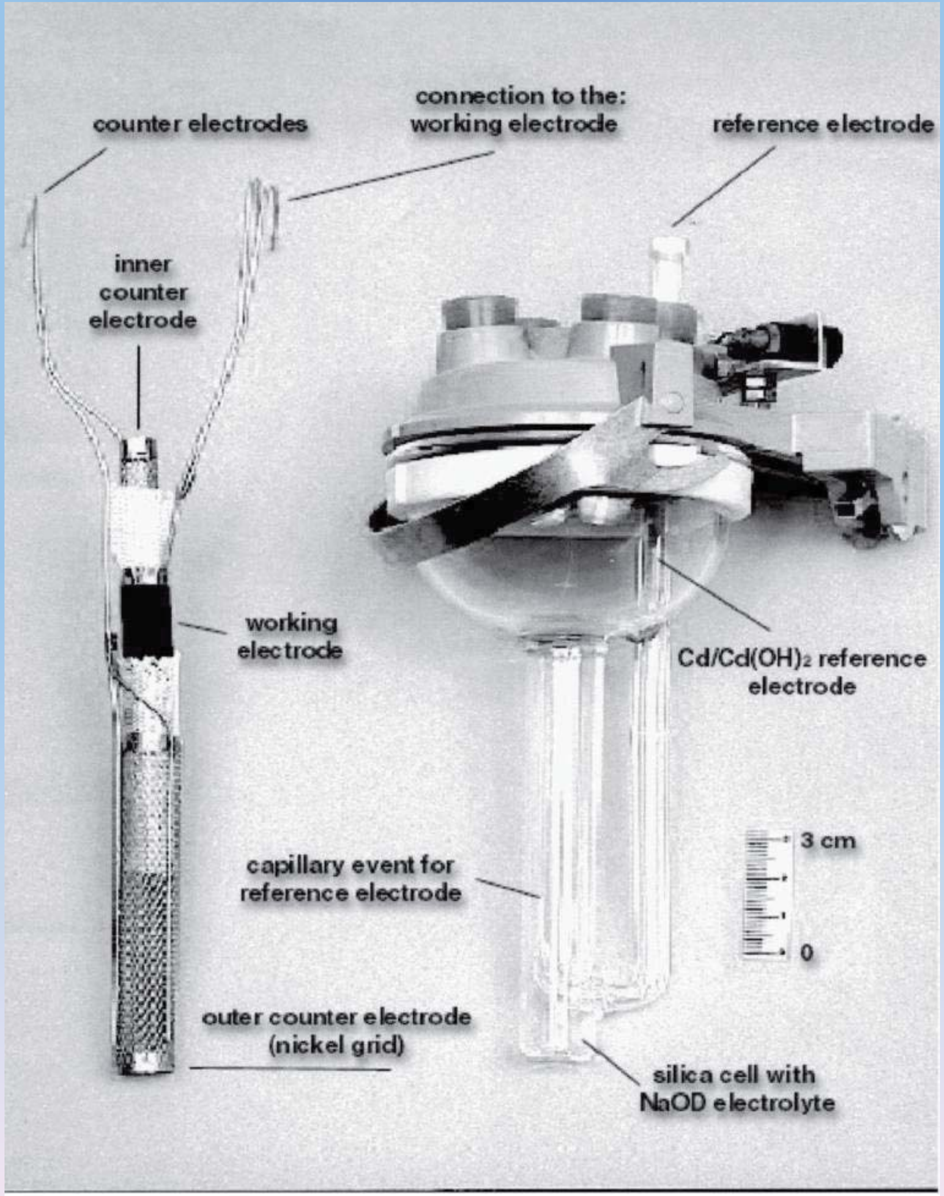

Fig. 3. View of the various parts of the in situ NPD electrochemical cell assembly.

Université du Québec
à Trois-Rivières

experimental

ILL, D20 high flux two-axis diffractometer

Position sensitive detector cover 160°

$\lambda = 2.41$Å

Flux $3.7X10^7$ n/s

Good paterns within 1 minute

$\Rightarrow$ Each pattern is a snapshot of the structural state of the electrode at this level of charge

$LaNi_5$

current density and electrochemical capacity

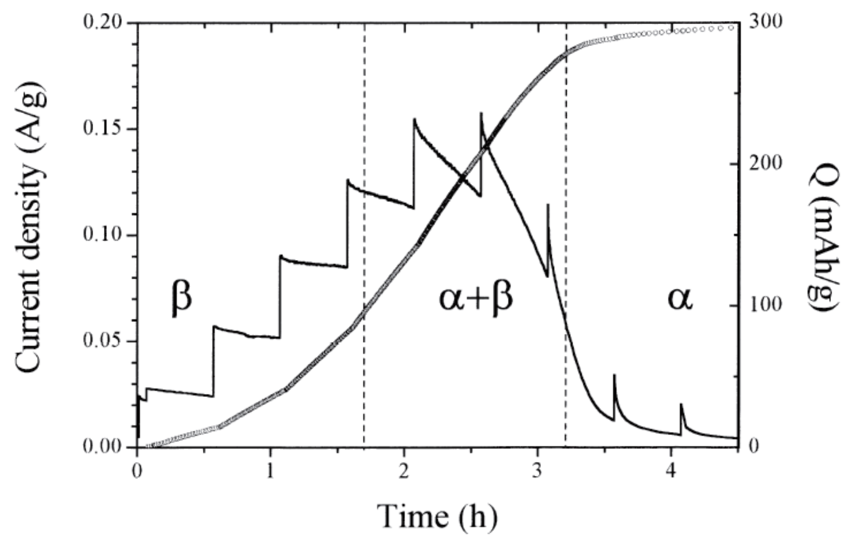

phase amount

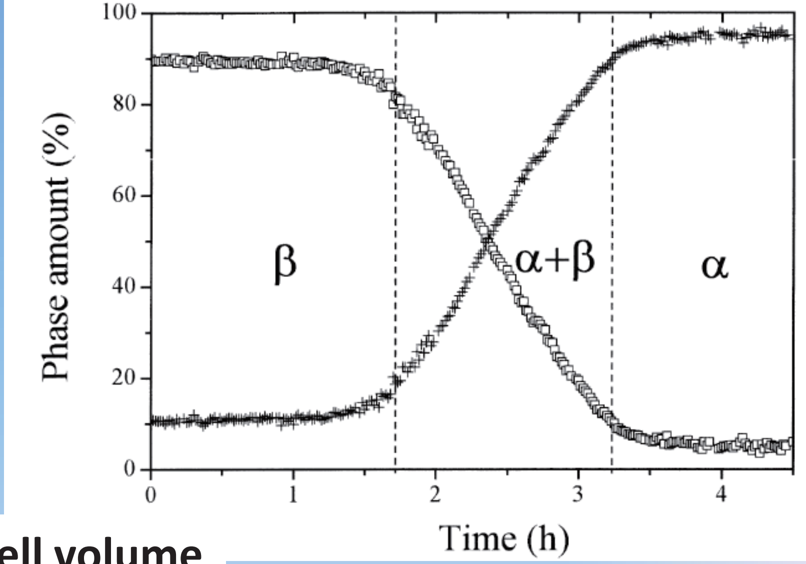

β phase cell volume

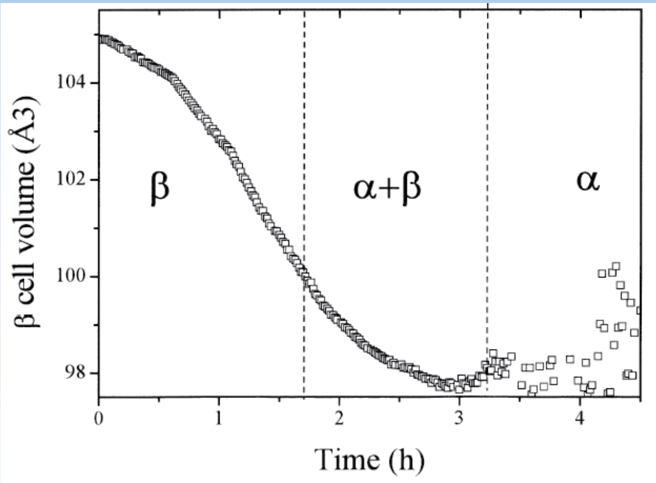

Neutron patterns

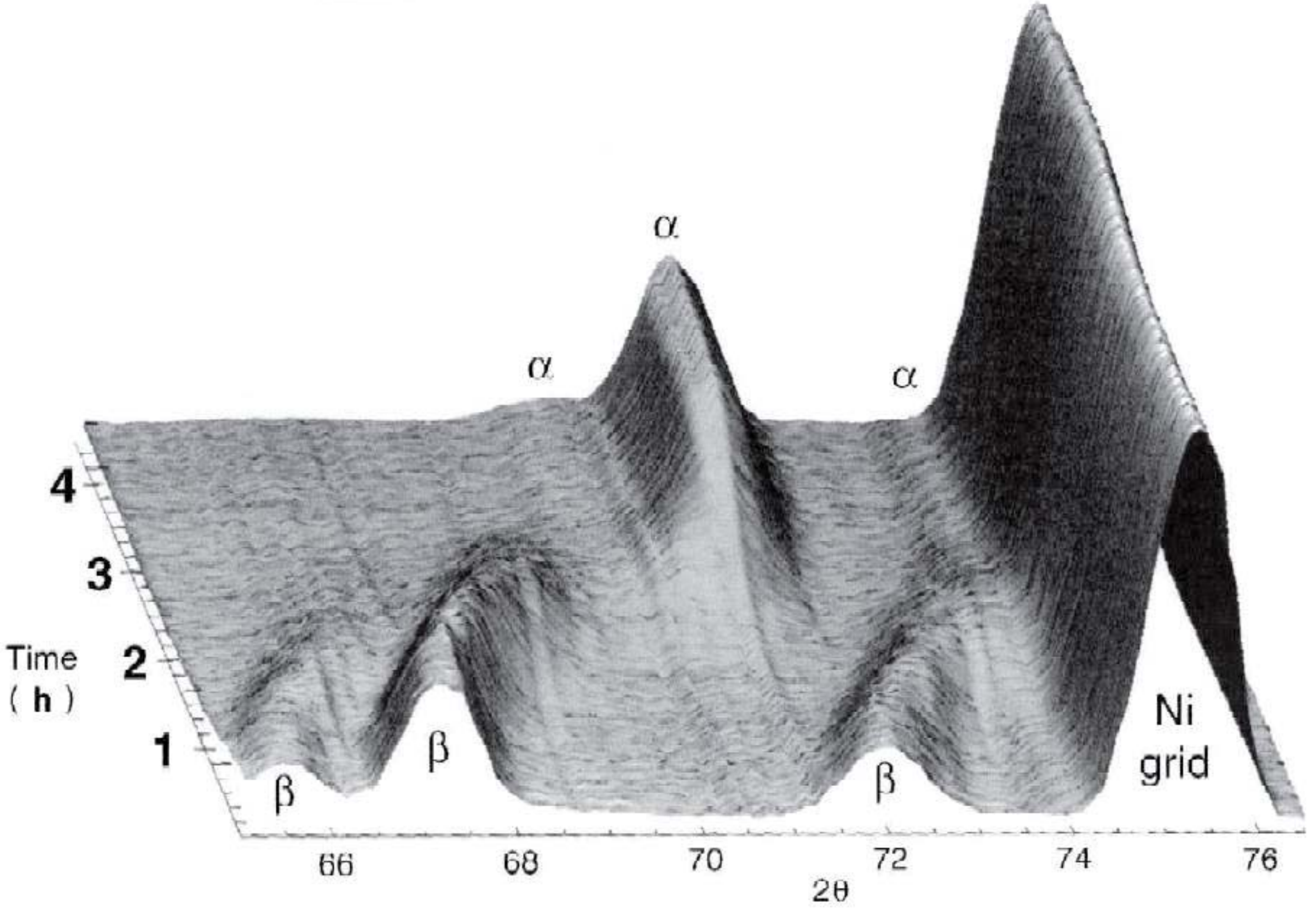

Fig. 4. 3D plot of the NPD patterns during a potentiodynamic discharge for the AT electrode.

Université du Québec
à Trois-Rivières

Structural behaviour

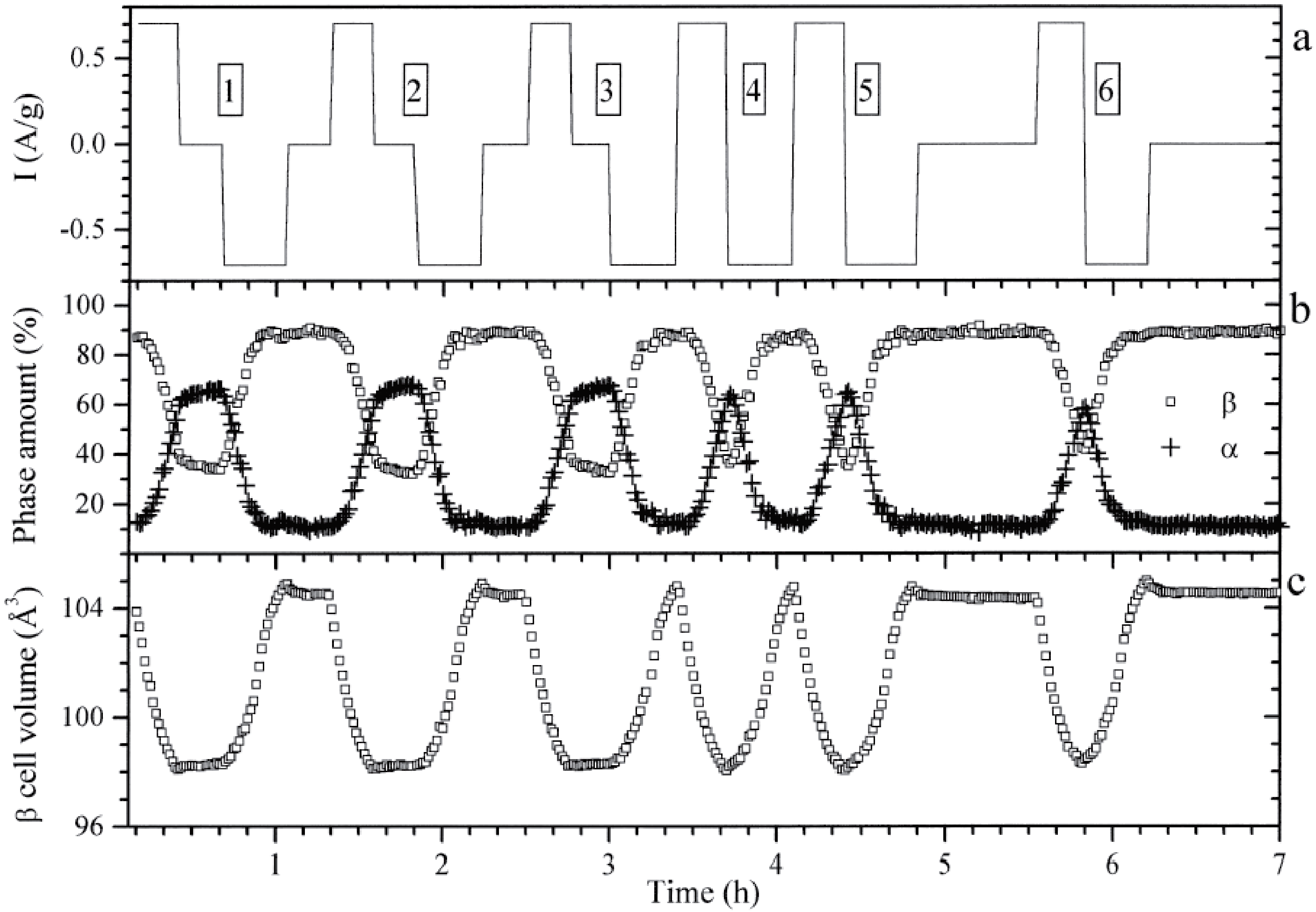

Fig. 8. Structural behaviour of the AT electrode under high rate (700 mA/g) discharge–charge cycles: (a) current densities; (b) phase amount; (c) cell volume.

Conclusion

- Surface treatment is essential to get a high capacity and fast kinetics

- On surface-treated electrodes, the kinetics of the structural modification (i.e. the mobility of the α/β interface) is the main limiting factor

BCC alloys

Solid solution BCC alloys (mainly Ti-V-Cr and Ti-V-Cr based) are promising hydrogen storage materials because of their relatively high storage capacity and their ability to absorb and desorb hydrogen in ambient conditions.

Question:

Upon substitution are there preferential sites for the atoms?

Neutron diffraction of the crystal structure of the multiphase alloy $TiMn_{1.1}V_{0.9}$.

Problem:

Scattering length

Ti = -3.370
V = -0.443
Mn = -3.750

⇒Refinement very hard

Could we still get some information?

BCC alloys

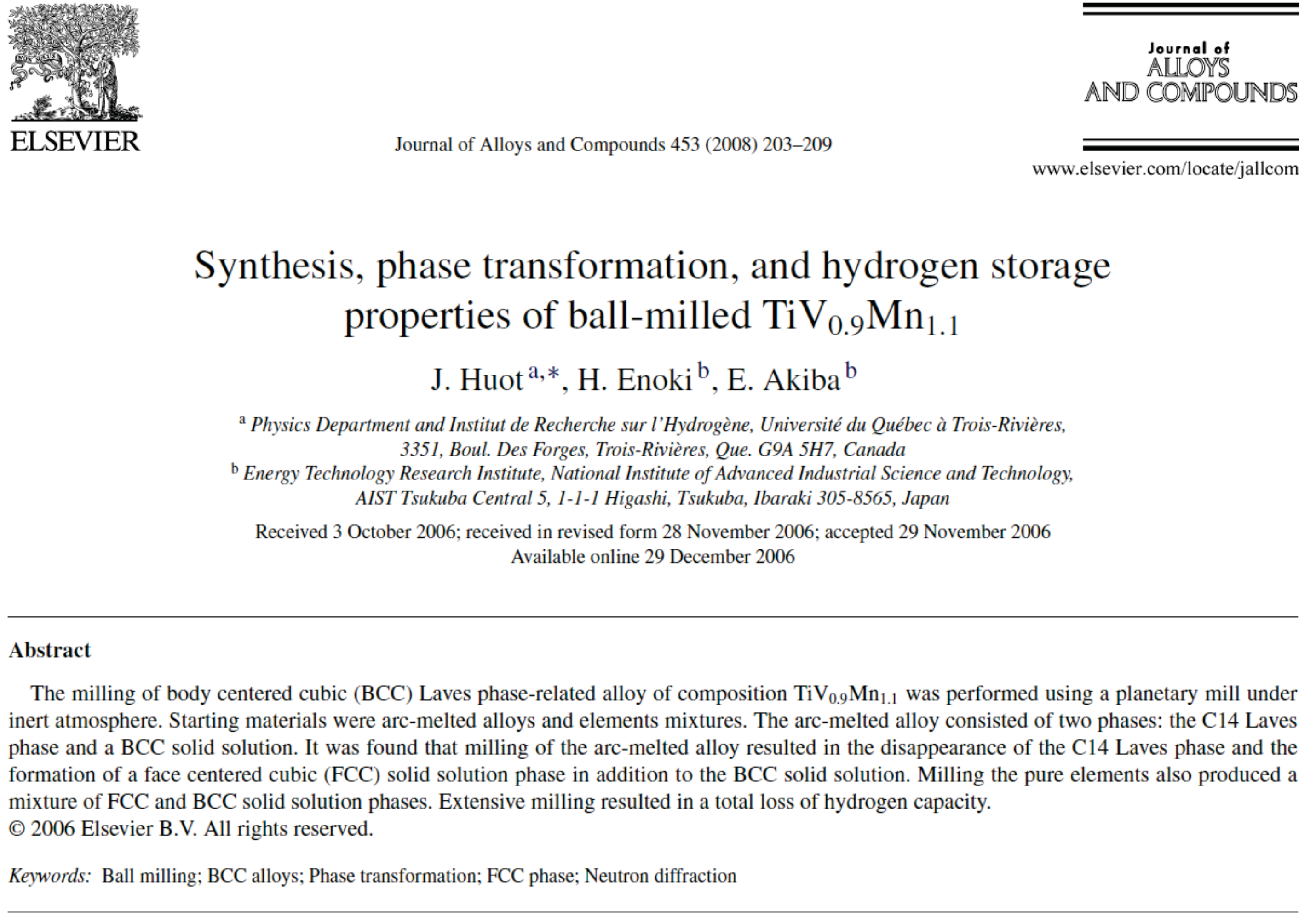

ELSEVIER

Journal of Alloys and Compounds 453 (2008) 203–209

Journal of ALLOYS AND COMPOUNDS

www.elsevier.com/locate/jallcom

Synthesis, phase transformation, and hydrogen storage properties of ball-milled $TiV_{0.9}Mn_{1.1}$

J. Huot[a,*], H. Enoki[b], E. Akiba[b]

[a] *Physics Department and Institut de Recherche sur l'Hydrogène, Université du Québec à Trois-Rivières,*
3351, Boul. Des Forges, Trois-Rivières, Que. G9A 5H7, Canada
[b] *Energy Technology Research Institute, National Institute of Advanced Industrial Science and Technology,*
AIST Tsukuba Central 5, 1-1-1 Higashi, Tsukuba, Ibaraki 305-8565, Japan

Received 3 October 2006; received in revised form 28 November 2006; accepted 29 November 2006
Available online 29 December 2006

Abstract

The milling of body centered cubic (BCC) Laves phase-related alloy of composition $TiV_{0.9}Mn_{1.1}$ was performed using a planetary mill under inert atmosphere. Starting materials were arc-melted alloys and elements mixtures. The arc-melted alloy consisted of two phases: the C14 Laves phase and a BCC solid solution. It was found that milling of the arc-melted alloy resulted in the disappearance of the C14 Laves phase and the formation of a face centered cubic (FCC) solid solution phase in addition to the BCC solid solution. Milling the pure elements also produced a mixture of FCC and BCC solid solution phases. Extensive milling resulted in a total loss of hydrogen capacity.

Keywords: Ball milling; BCC alloys; Phase transformation; FCC phase; Neutron diffraction

---

Neutron diffraction pattern and Rietveld refinement of $TiV_{0.9}Mn_{1.1}$

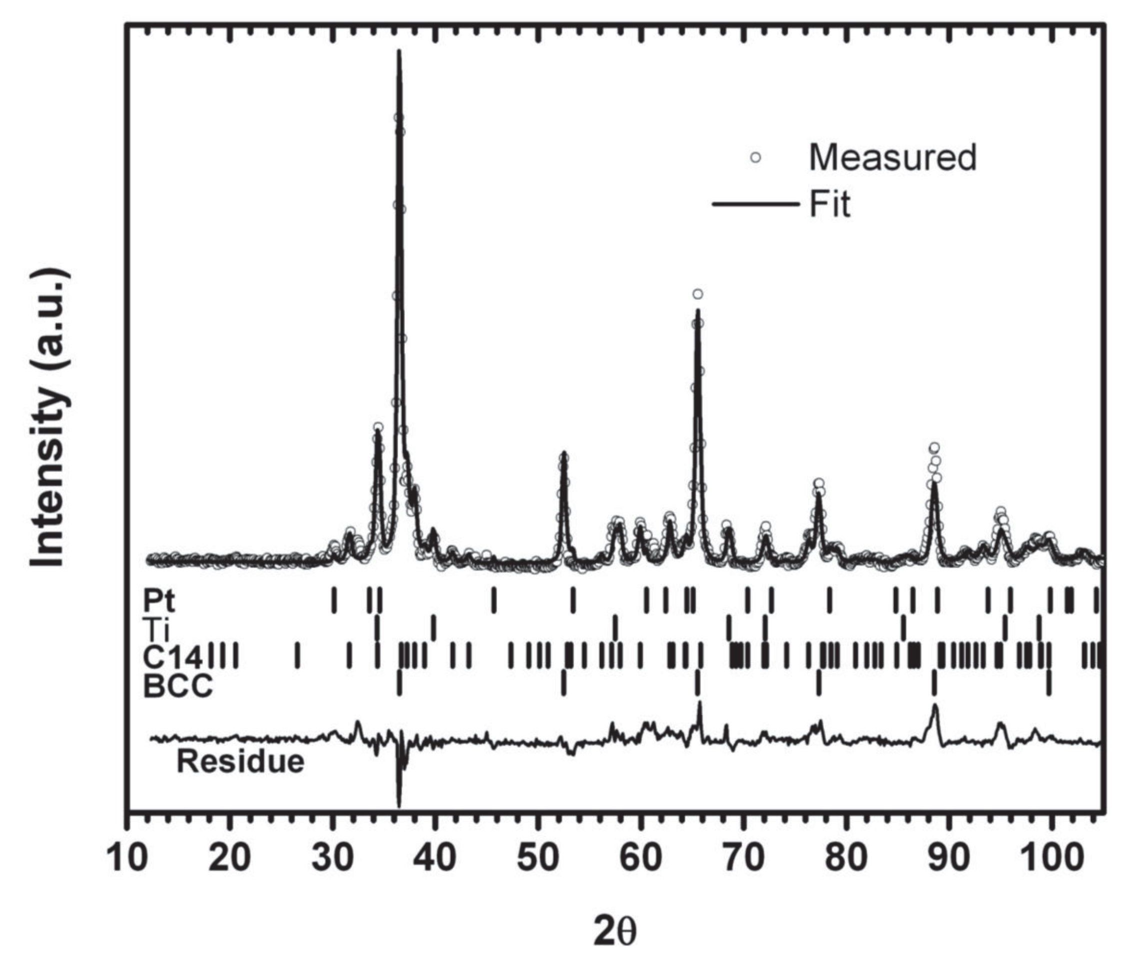

Université du Québec
à Trois-Rivières

Crystal structure

Phase	Space Group	Abundance (%)	Lattice parameters (Å)
C14	P 6_3/mmc	32 (4)	*a* =4.906(3) *c* = 8.011(9)
BCC	I m -3 m	65 (1)	*a* =3.018(1)
Titanium	P 6_3/mmc	3 (1)	*a* =2.971(5) *c* = 4.63(1)

UQTR
Université du Québec
à Trois-Rivières

Crystallographic parameters, C14 phase

Site (Wickoff symbol)	Refined Coordinates	Atoms	Occupancy
2*a*	--	Mn V	0.65 0.35
4*f*	z = 0.065	Ti	1.0
6*h*	x = 0.82356	Mn V	0.58 0.42

Conclusion

Titanium atoms are localized exclusively on the *4f* site while the manganese and vanadium atoms are distributed on the 2*a* and 6*h* sites but with a different abundance.

These abundances give a stoichiometry of $TiV_{0.8}Mn_{1.2}$ for the C14 phase.

$TiV_{1.1}Mn_{0.9}$

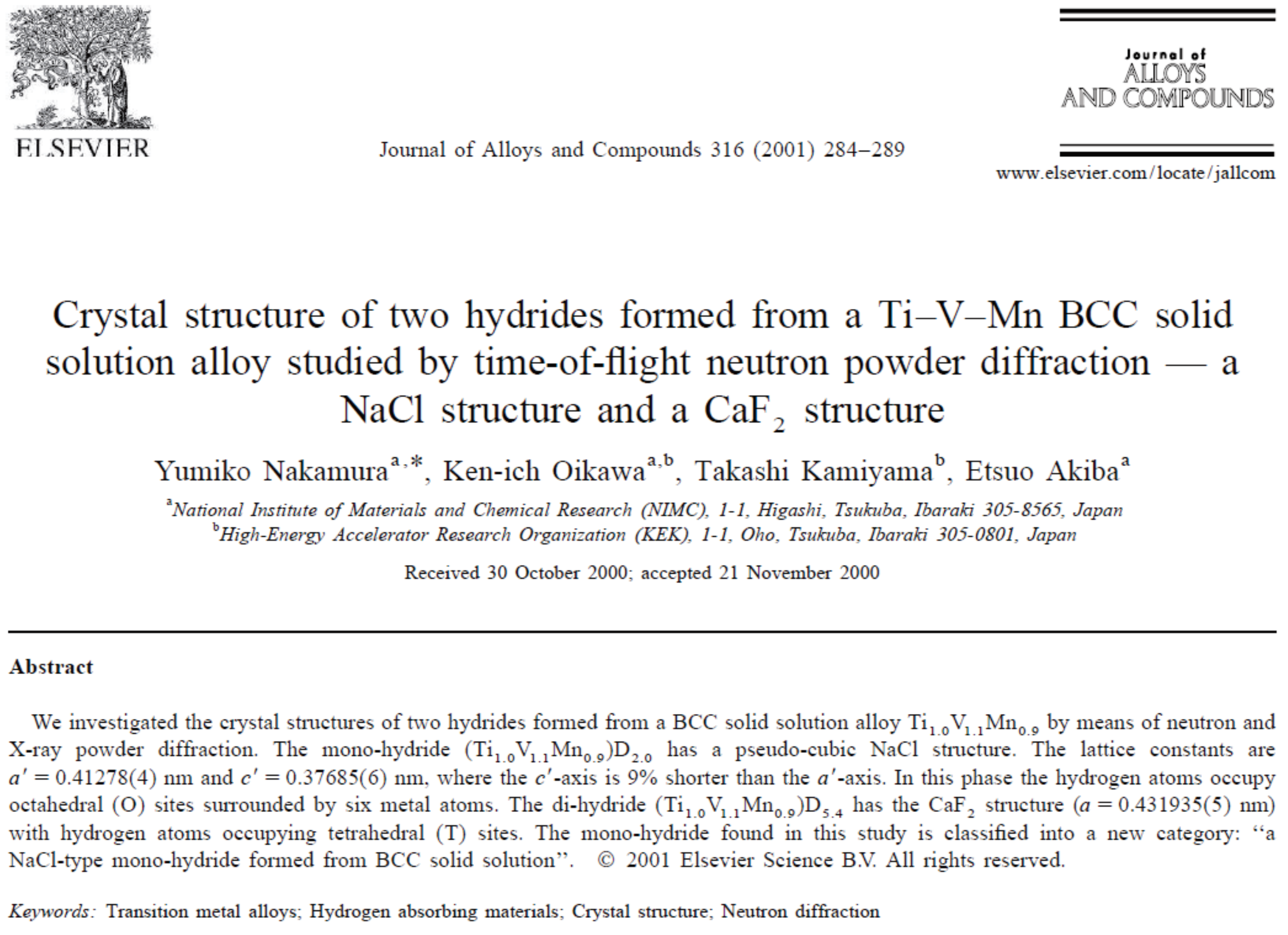

ELSEVIER

Journal of Alloys and Compounds 316 (2001) 284–289

Journal of ALLOYS AND COMPOUNDS

www.elsevier.com/locate/jallcom

Crystal structure of two hydrides formed from a Ti–V–Mn BCC solid solution alloy studied by time-of-flight neutron powder diffraction — a NaCl structure and a CaF_2 structure

Yumiko Nakamura[a,*], Ken-ich Oikawa[a,b], Takashi Kamiyama[b], Etsuo Akiba[a]

[a] *National Institute of Materials and Chemical Research (NIMC), 1-1, Higashi, Tsukuba, Ibaraki 305-8565, Japan*
[b] *High-Energy Accelerator Research Organization (KEK), 1-1, Oho, Tsukuba, Ibaraki 305-0801, Japan*

Received 30 October 2000; accepted 21 November 2000

Abstract

We investigated the crystal structures of two hydrides formed from a BCC solid solution alloy $Ti_{1.0}V_{1.1}Mn_{0.9}$ by means of neutron and X-ray powder diffraction. The mono-hydride $(Ti_{1.0}V_{1.1}Mn_{0.9})D_{2.0}$ has a pseudo-cubic NaCl structure. The lattice constants are $a' = 0.41278(4)$ nm and $c' = 0.37685(6)$ nm, where the c'-axis is 9% shorter than the a'-axis. In this phase the hydrogen atoms occupy octahedral (O) sites surrounded by six metal atoms. The di-hydride $(Ti_{1.0}V_{1.1}Mn_{0.9})D_{5.4}$ has the CaF_2 structure ($a = 0.431935(5)$ nm) with hydrogen atoms occupying tetrahedral (T) sites. The mono-hydride found in this study is classified into a new category: "a NaCl-type mono-hydride formed from BCC solid solution".

Keywords: Transition metal alloys; Hydrogen absorbing materials; Crystal structure; Neutron diffraction

Find the crystal structures of mono- and di-hydrides

PCT at 313K

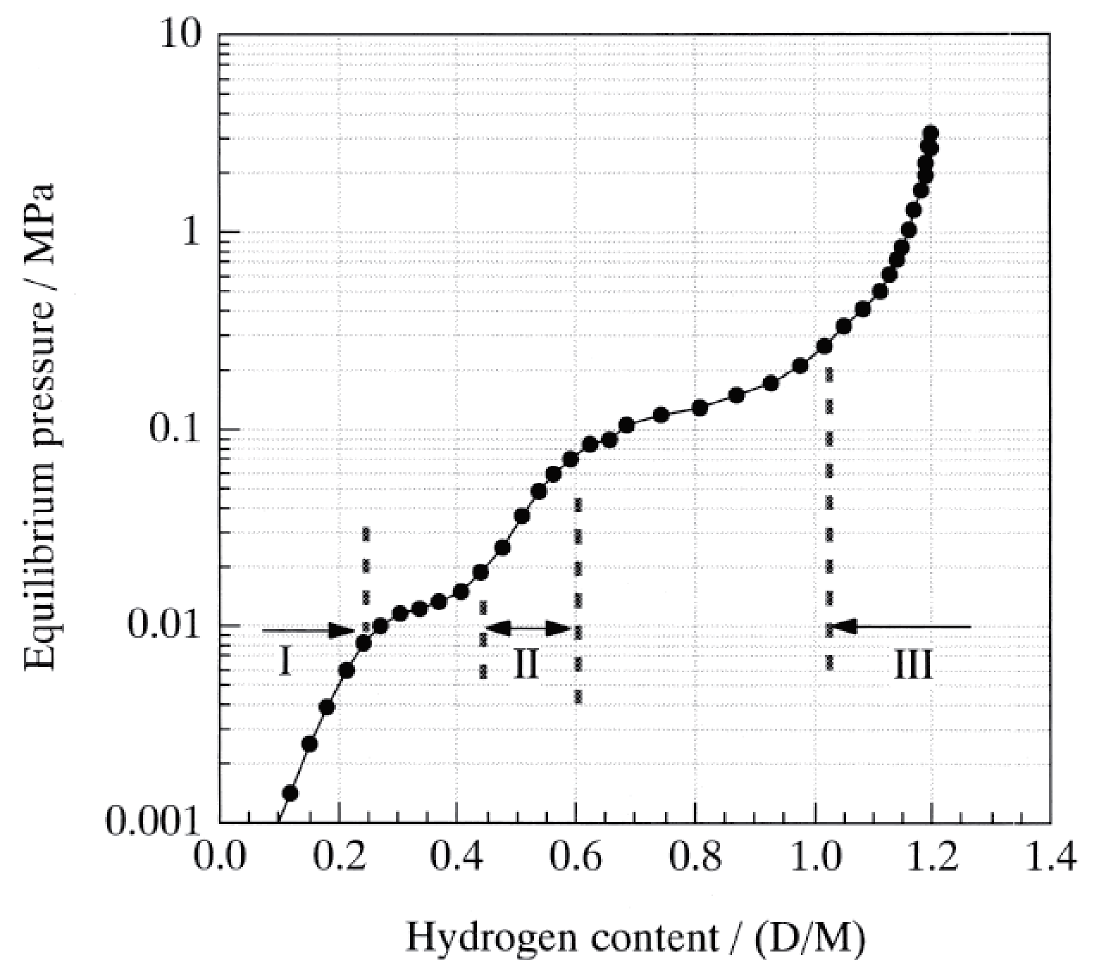

(I) distorted BCC phase

(II) deformed (pseudo-cubic) FCC phase,

(III) FCC phase

Université du Québec
à Trois-Rivières

Experimental

- Room temperature
- Backward bank of time-of-flight (TOF) diffractometer, *Vega at the Neutron Science* Laboratory (KENS) of the High Energy Accelerator Research Organization (KEK), Tsukuba, Japan.

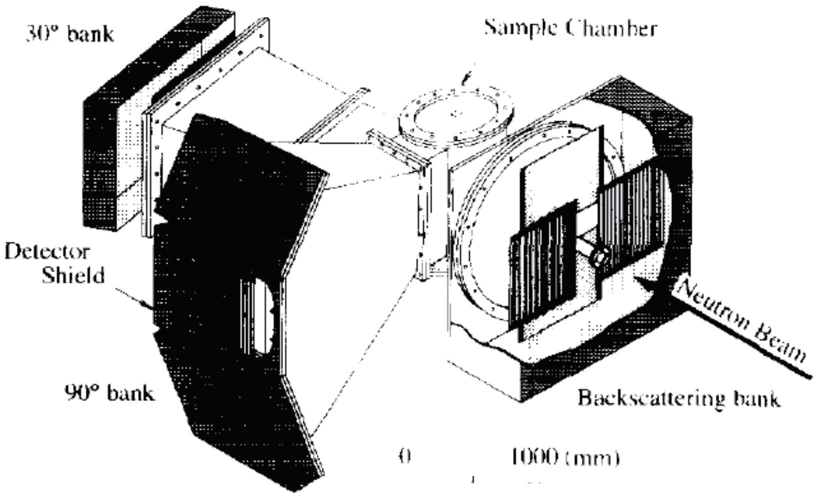

Fig. 1. Three-dimensional view of the TOF powder diffractometer VEGA.

$TiV_{1.1}Mn_{0.9}D_{5.4}$

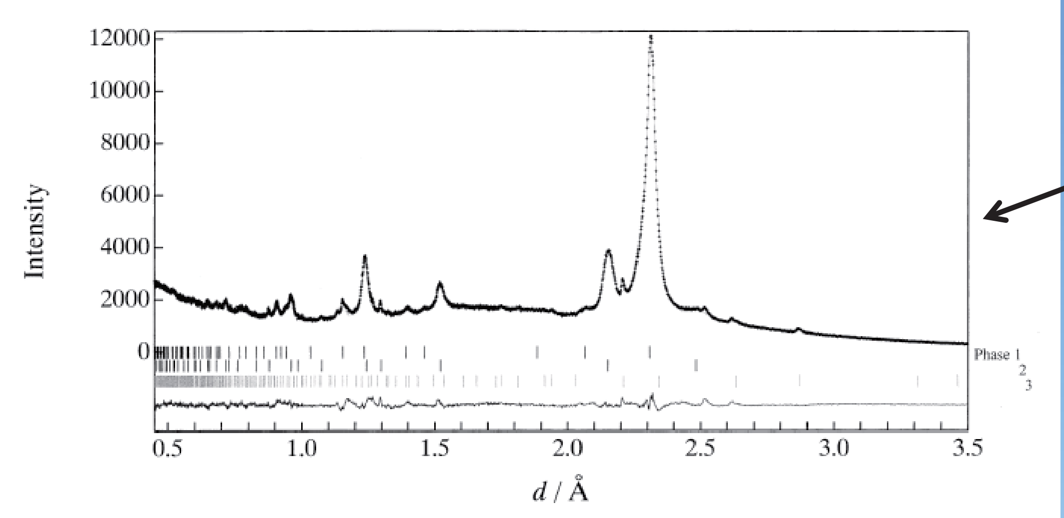

Mono-hydride

Fit: Mono-hydride, di-hydride, $Zr_3V_3OD_x$

Di-hydride

Fit: Mono-hydride, di-hydride, $Zr_3V_3OD_x$

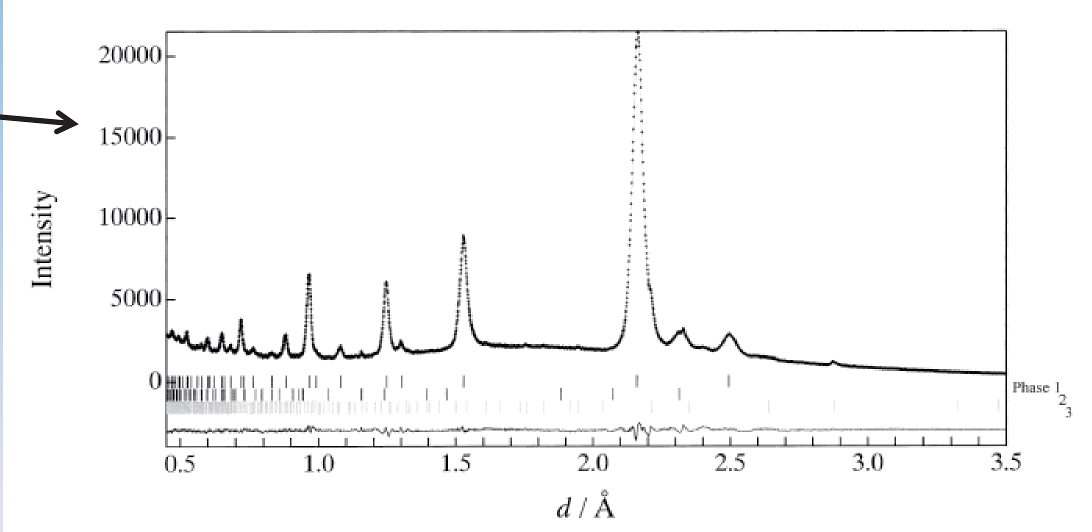

Rietveld results mono-hydride

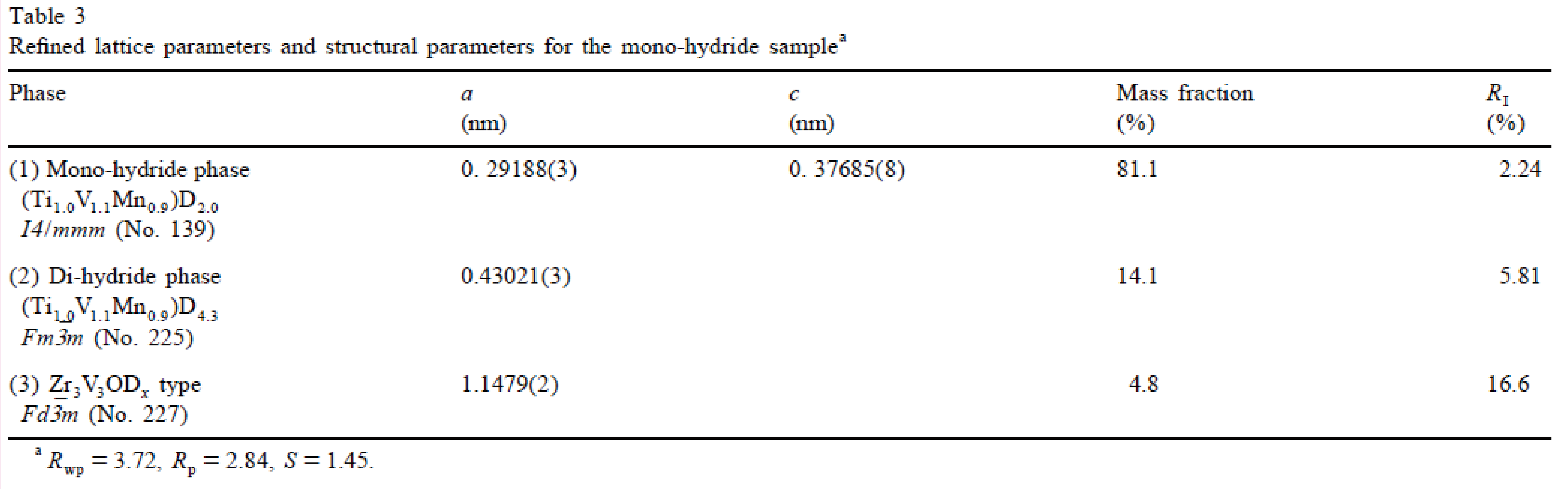

Table 3

Refined lattice parameters and structural parameters for the mono-hydride sample[a]

Phase	a (nm)	c (nm)	Mass fraction (%)	R_I (%)
(1) Mono-hydride phase $(Ti_{1.0}V_{1.1}Mn_{0.9})D_{2.0}$ $I4/mmm$ (No. 139)	0. 29188(3)	0. 37685(8)	81.1	2.24
(2) Di-hydride phase $(Ti_{1.0}V_{1.1}Mn_{0.9})D_{4.3}$ $Fm3m$ (No. 225)	0.43021(3)		14.1	5.81
(3) $Zr_3V_3OD_x$ type $Fd\bar{3}m$ (No. 227)	1.1479(2)		4.8	16.6

[a] $R_{wp} = 3.72$, $R_p = 2.84$, $S = 1.45$.

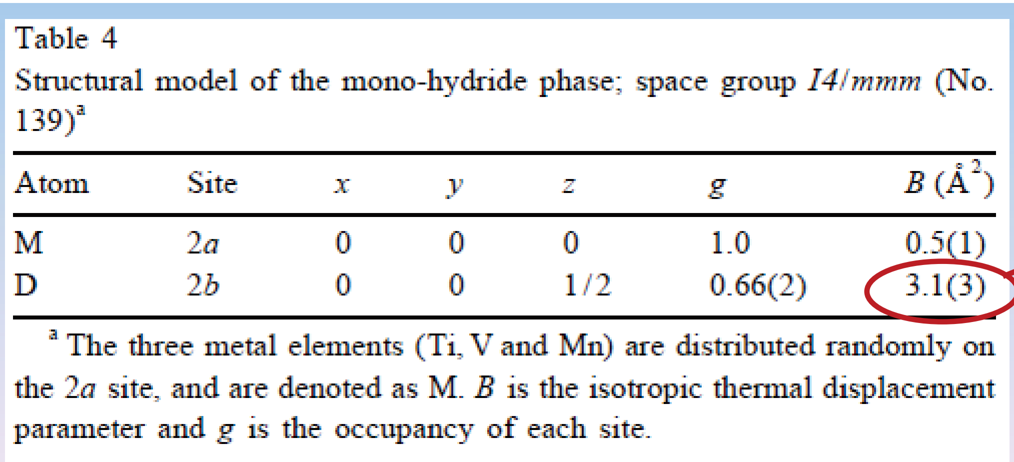

Table 4

Structural model of the mono-hydride phase; space group $I4/mmm$ (No. 139)[a]

Atom	Site	x	y	z	g	B (Å^2)
M	2a	0	0	0	1.0	0.5(1)
D	2b	0	0	1/2	0.66(2)	3.1(3)

[a] The three metal elements (Ti, V and Mn) are distributed randomly on the 2a site, and are denoted as M. B is the isotropic thermal displacement parameter and g is the occupancy of each site.

local distortion
or disorder

Rietveld results di-hydride

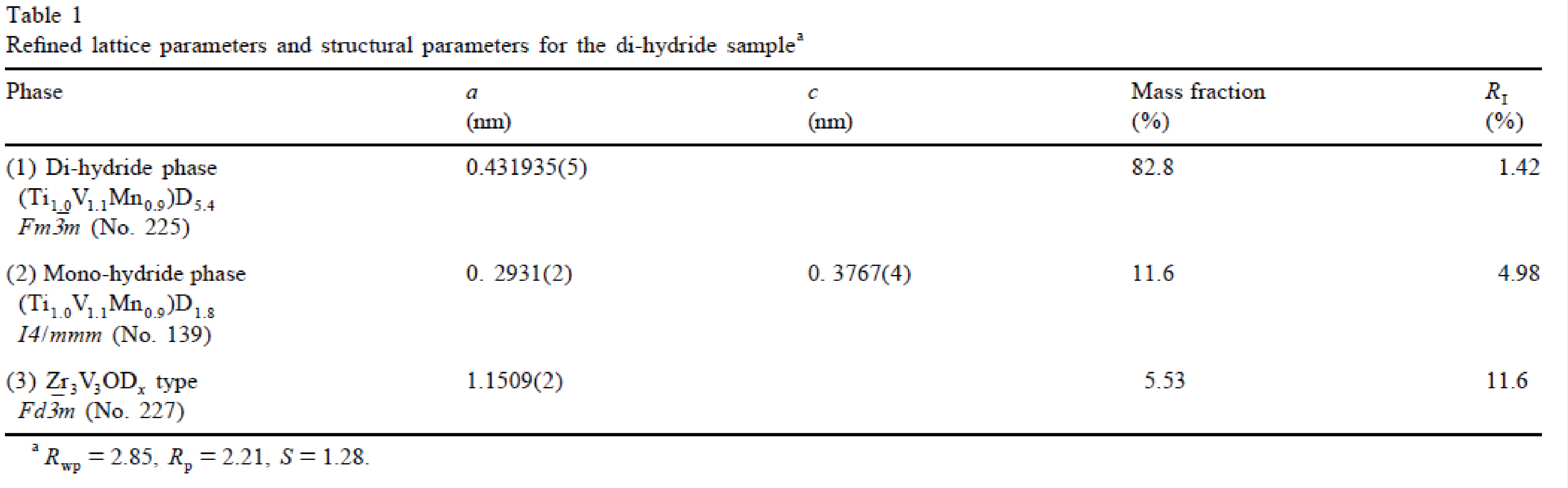

Table 1
Refined lattice parameters and structural parameters for the di-hydride sample[a]

Phase	a (nm)	c (nm)	Mass fraction (%)	R_I (%)
(1) Di-hydride phase $(Ti_{1.0}V_{1.1}Mn_{0.9})D_{5.4}$ $Fm\bar{3}m$ (No. 225)	0.431935(5)		82.8	1.42
(2) Mono-hydride phase $(Ti_{1.0}V_{1.1}Mn_{0.9})D_{1.8}$ $I4/mmm$ (No. 139)	0. 2931(2)	0. 3767(4)	11.6	4.98
(3) $Zr_3V_3OD_x$ type $Fd\bar{3}m$ (No. 227)	1.1509(2)		5.53	11.6

[a] $R_{wp} = 2.85$, $R_p = 2.21$, $S = 1.28$.

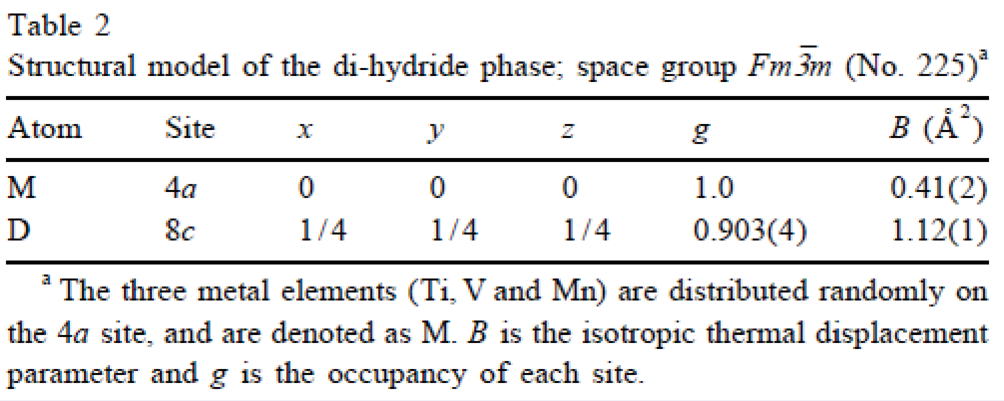

Table 2
Structural model of the di-hydride phase; space group $Fm\bar{3}m$ (No. 225)[a]

Atom	Site	x	y	z	g	B (Å^2)
M	4*a*	0	0	0	1.0	0.41(2)
D	8*c*	1/4	1/4	1/4	0.903(4)	1.12(1)

[a] The three metal elements (Ti, V and Mn) are distributed randomly on the 4*a* site, and are denoted as M. *B* is the isotropic thermal displacement parameter and *g* is the occupancy of each site.

UQTR
Université du Québec
à Trois-Rivières

Mono and di-hydride structures

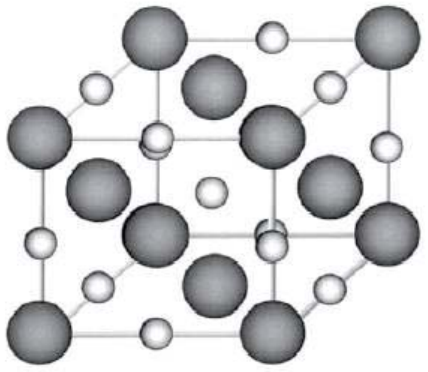

Fig. 5. Crystal structure of the mono-hydride phase $(\mathrm{Ti}_{1.0}\mathrm{V}_{1.1}\mathrm{Mn}_{0.9})\mathrm{D}_{2.0}$. Large and small spheres indicate metal atoms and hydrogen atoms, respectively.

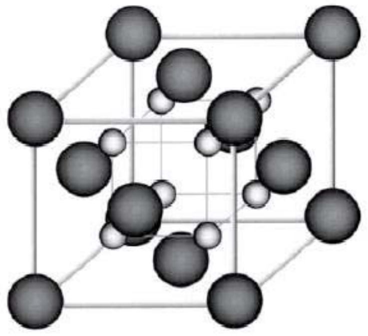

Fig. 3. Crystal structure of the di-hydride phase $(\mathrm{Ti}_{1.0}\mathrm{V}_{1.1}\mathrm{Mn}_{0.9})\mathrm{D}_{5.4}$. Large and small spheres indicate metal atoms and hydrogen atoms, respectively.

Empirical threshold for hydrogen accommodation: r ≈ 0.04nm

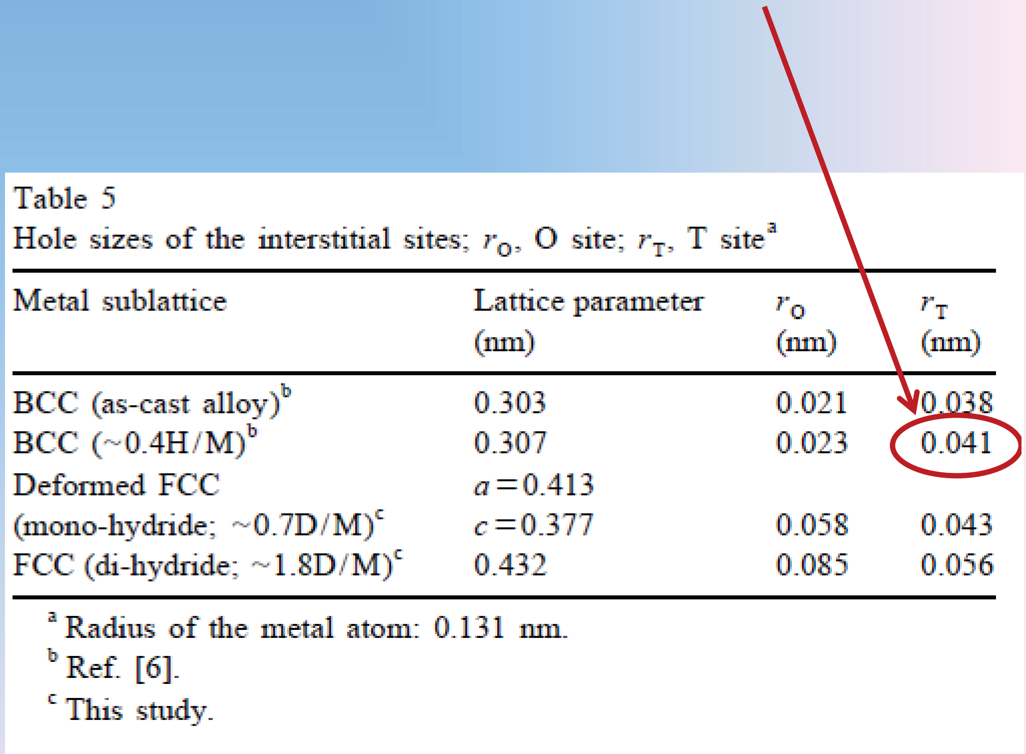

Table 5
Hole sizes of the interstitial sites; r_O, O site; r_T, T site[a]

Metal sublattice	Lattice parameter (nm)	r_O (nm)	r_T (nm)
BCC (as-cast alloy)[b]	0.303	0.021	0.038
BCC (~0.4H/M)[b]	0.307	0.023	0.041
Deformed FCC	$a=0.413$		
(mono-hydride; ~0.7D/M)[c]	$c=0.377$	0.058	0.043
FCC (di-hydride; ~1.8D/M)[c]	0.432	0.085	0.056

[a] Radius of the metal atom: 0.131 nm.
[b] Ref. [6].
[c] This study.

Conclusions

The mono-hydride phase $(TiV_{1.1}Mn_{0.9})D_{2.0}$ has a pseudo-cubic NaCl structure, one axis of which is reduced by about 9%. It is classified into a new category: ‘‘a NaCl-type mono-hydride formed from BCC solid solution’’.

The di-hydride phase $(TiV_{1.1}Mn_{0.9})D_{5.4}$ has a CaF_2 structure as found in di-hydrides of BCC metals such as V and Nb.

This shows that BCC metals and BCC solid-solution alloys form a NaCl-type hydride under appropriate conditions.

Complex hydrides

- **High capacities**
- **Thermodynamic reasonable**
- **Main problems:**
    - **Reversibility, kinetics, cost, safety**

Example: $NaAlH_4$

$NaAlD_4$

In 1997 Bogdanovic and Schwickardi showed that hydrogenation/dehydrogenation of $NaAlH_4$ is reversible when doped with Ti-based compounds.

Reversible capacity ≈ 5.6 wt.%

Much work has been done on this system

Some discrepancies between Al-H bond distance measured from IR and X-ray diffraction.

Hydrogen could be located with neutron

$NaAlD_4$

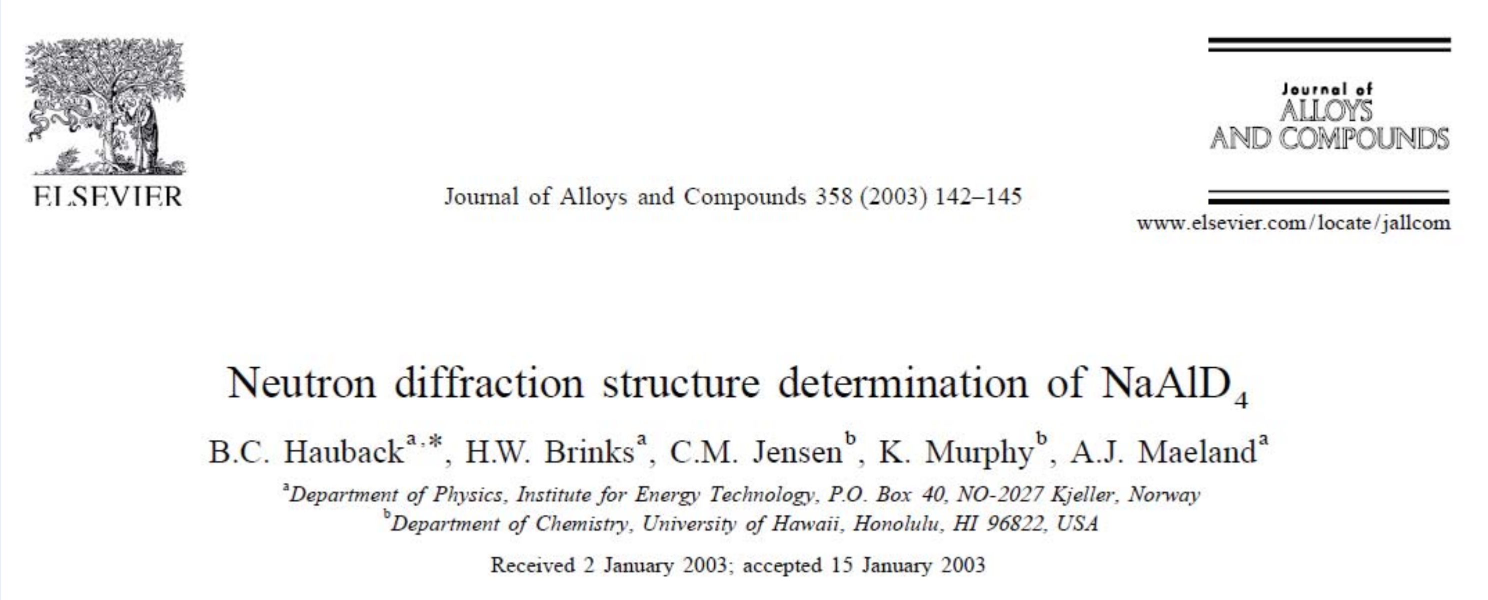

ELSEVIER

Journal of Alloys and Compounds 358 (2003) 142–145

Journal of
ALLOYS
AND COMPOUNDS

www.elsevier.com/locate/jallcom

Neutron diffraction structure determination of $NaAlD_4$

B.C. Hauback[a,*], H.W. Brinks[a], C.M. Jensen[b], K. Murphy[b], A.J. Maeland[a]

[a] *Department of Physics, Institute for Energy Technology, P.O. Box 40, NO-2027 Kjeller, Norway*
[b] *Department of Chemistry, University of Hawaii, Honolulu, HI 96822, USA*

Received 2 January 2003; accepted 15 January 2003

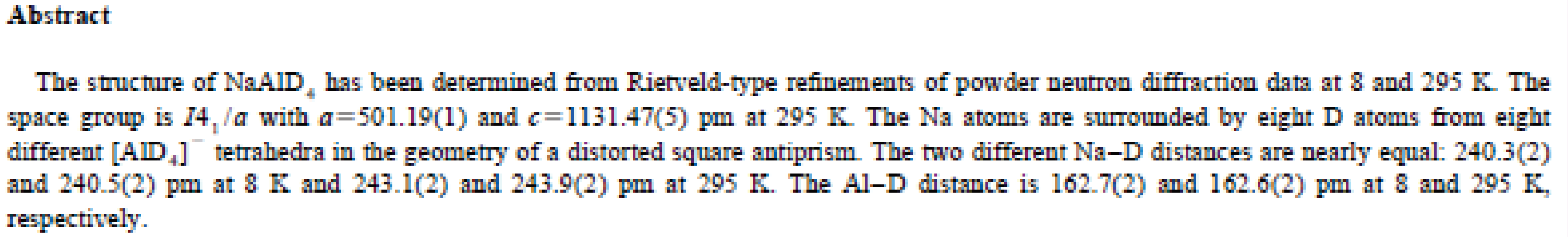

Abstract

The structure of $NaAlD_4$ has been determined from Rietveld-type refinements of powder neutron diffraction data at 8 and 295 K. The space group is $I4_1/a$ with $a=501.19(1)$ and $c=1131.47(5)$ pm at 295 K. The Na atoms are surrounded by eight D atoms from eight different $[AlD_4]^-$ tetrahedra in the geometry of a distorted square antiprism. The two different Na–D distances are nearly equal: 240.3(2) and 240.5(2) pm at 8 K and 243.1(2) and 243.9(2) pm at 295 K. The Al–D distance is 162.7(2) and 162.6(2) pm at 8 and 295 K, respectively.

Experimental

$NaAlD_4$ (99% pure) contained significant amounts of NaF and Al impurities.

Powder neutron diffraction (PND) data at 8 and 295 K collected with PUS diffractometer at the JEEP II reactor at Kjeller, Norway

Monochromatic neutrons with wavelength 155.46 nm

Cylindrical vanadium sample holder of 5 mm diameter.
Sample was rotated at 295K but not at 8K.

The regions 2θ 46.00–46.75°, 76.50–77.60° and 116.00–117.30° were excluded in the analysis of the PND data at 8 K due to additional scattering from the Displex cooling system.

UQTR
Université du Québec
à Trois-Rivières

$NaAlD_4$

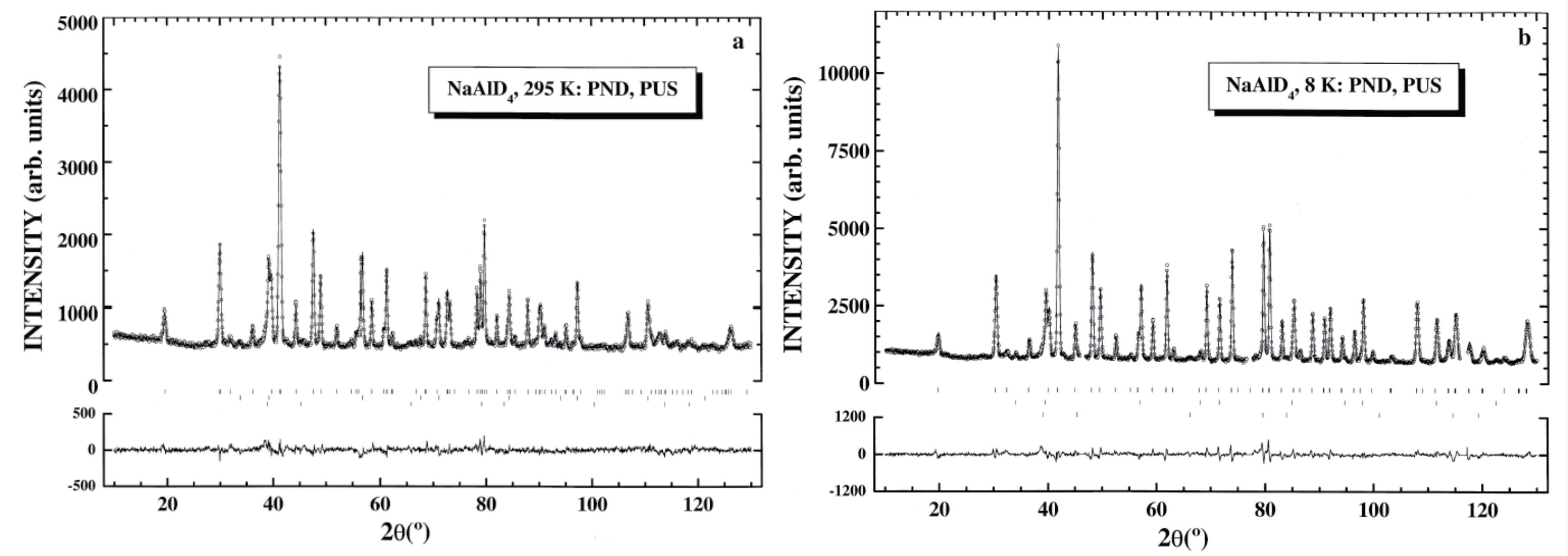

From Rietveld refinement: 57 wt% $NaAlD_4$, 29 wt% NaF and 14wt% Al.

Results

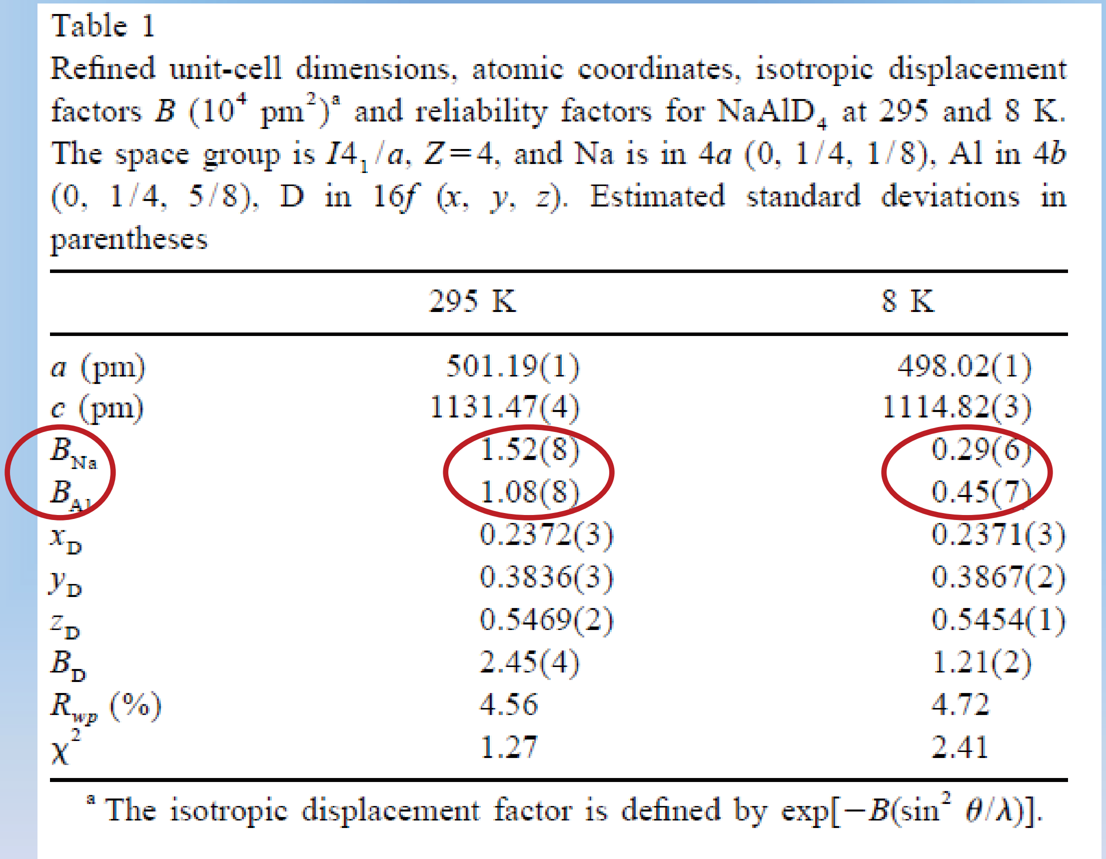

Table 1

Refined unit-cell dimensions, atomic coordinates, isotropic displacement factors B (10^4 pm^2)^a and reliability factors for $NaAlD_4$ at 295 and 8 K. The space group is $I4_1/a$, $Z=4$, and Na is in $4a$ (0, 1/4, 1/8), Al in $4b$ (0, 1/4, 5/8), D in $16f$ (x, y, z). Estimated standard deviations in parentheses

	295 K	8 K
a (pm)	501.19(1)	498.02(1)
c (pm)	1131.47(4)	1114.82(3)
B_{Na}	1.52(8)	0.29(6)
B_{Al}	1.08(8)	0.45(7)
x_D	0.2372(3)	0.2371(3)
y_D	0.3836(3)	0.3867(2)
z_D	0.5469(2)	0.5454(1)
B_D	2.45(4)	1.21(2)
R_{wp} (%)	4.56	4.72
χ^2	1.27	2.41

[a] The isotropic displacement factor is defined by $\exp[-B(\sin^2\theta/\lambda)]$.

Université du Québec
à Trois-Rivières

Results

- Shrinkage of the tetragonal unit cell larger along crystallographic *c*-axis (1.5%) than *a* axis (0.6%)

- Displacement parameter for deuterium relatively large at 295 K.

- High thermal motion possibly related to the low thermal stability of $NaAlD_4$

Inter-atomic distances

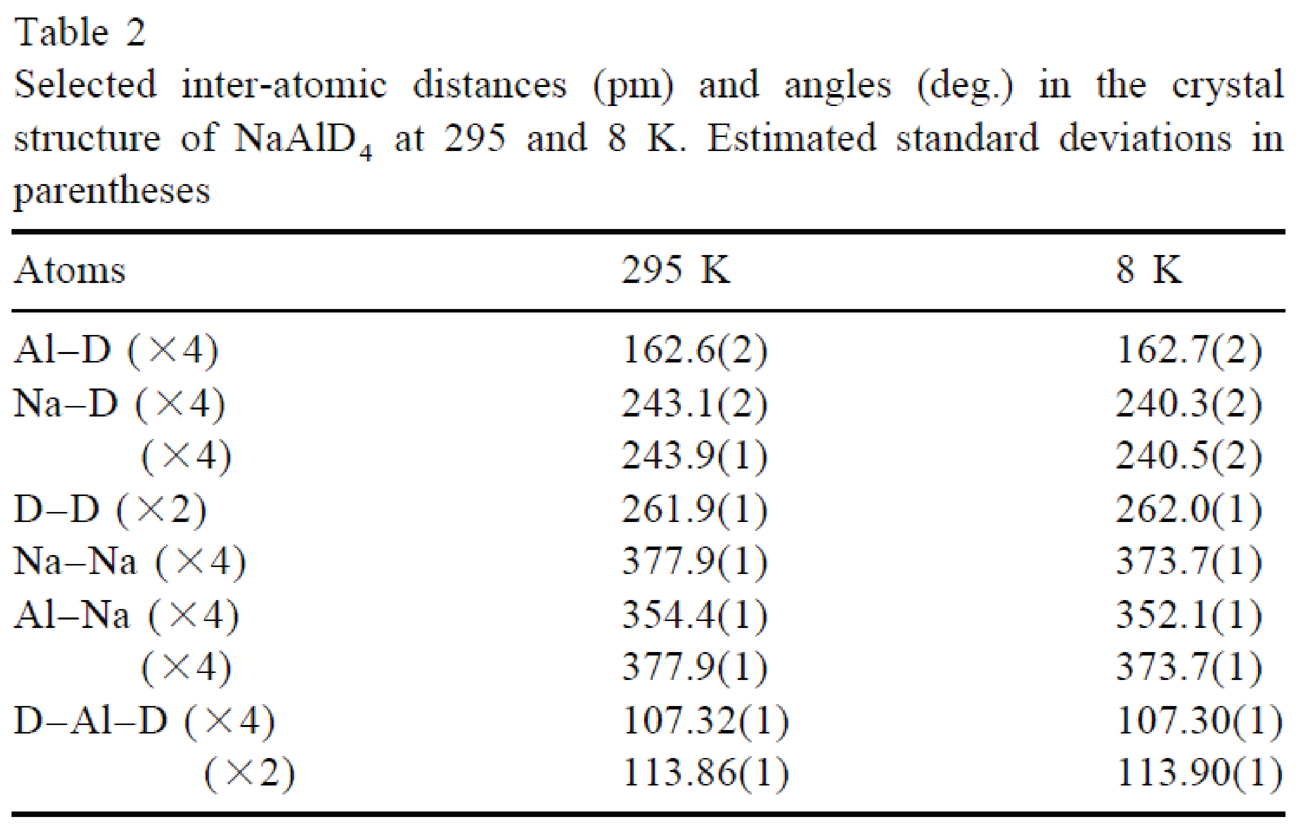

Table 2
Selected inter-atomic distances (pm) and angles (deg.) in the crystal structure of $NaAlD_4$ at 295 and 8 K. Estimated standard deviations in parentheses

Atoms	295 K	8 K
Al–D (×4)	162.6(2)	162.7(2)
Na–D (×4)	243.1(2)	240.3(2)
(×4)	243.9(1)	240.5(2)
D–D (×2)	261.9(1)	262.0(1)
Na–Na (×4)	377.9(1)	373.7(1)
Al–Na (×4)	354.4(1)	352.1(1)
(×4)	377.9(1)	373.7(1)
D–Al–D (×4)	107.32(1)	107.30(1)
(×2)	113.86(1)	113.90(1)

Results

Structure is isolated [AlD4] $^{-}$ tetrahedra connected via Na atoms.

If the Al–D bonds in neighbouring tetrahedra were pointed directly towards each other, the D–D distance would have been as low as 52.7 pm, but the tetrahedra are in fact oriented with all four faces pointed towards neighbouring tetrahedra.

The D–D distances are thereby maximized

the Al–D distances do not change on cooling from 295 to 8 K.

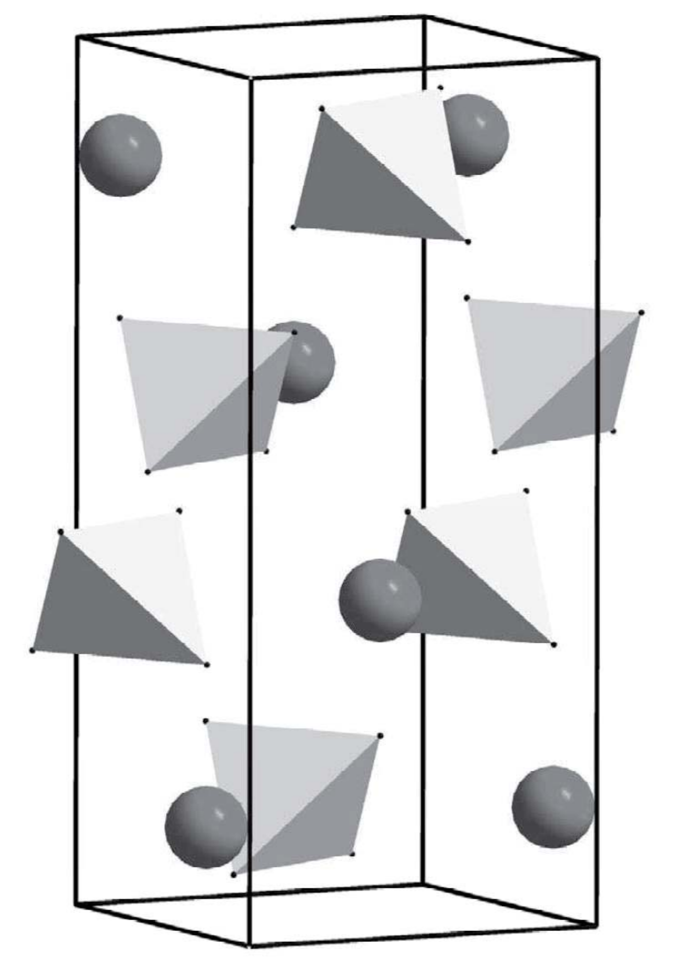

Fig. 2. The crystal structure of $NaAlD_4$. $[AlD_4]^-$ tetrahedra are linked via Na atoms.

UQTR
Université du Québec à Trois-Rivières

Results

Each Na atom has eight D atoms as nearest neighbours, each from different [AlD_4] tetrahedra, in the geometry of a distorted square antiprism.

Shortest D–D distances at 295 K of 261.9(1) pm are found within tetrahedron.

Shortest D–D distance between different tetrahedra is slightly larger 271.9(1) pm.

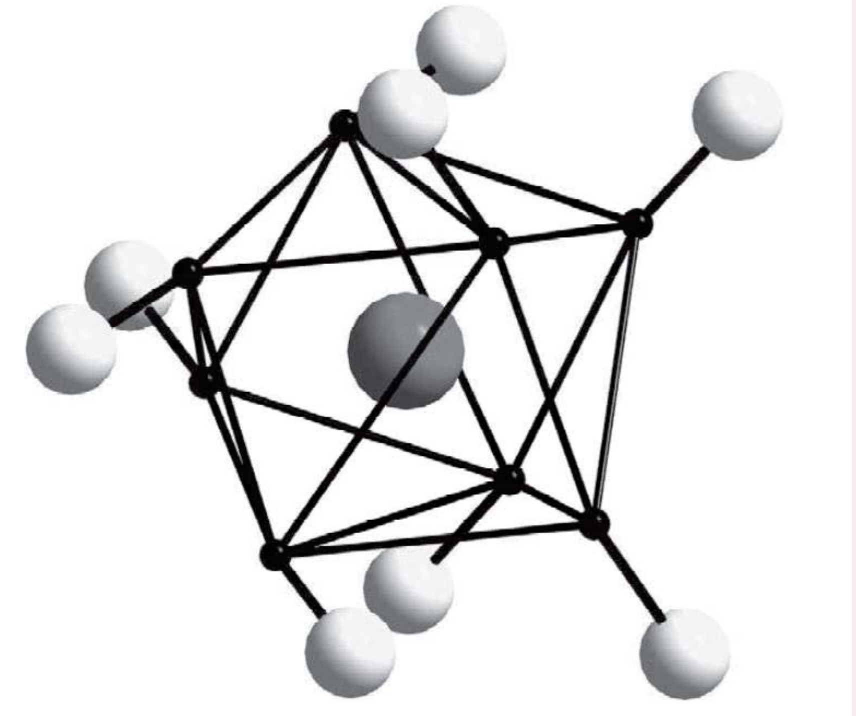

Fig. 3. Each Na atom is connected to eight $[AlD_4]^-$ tetrahedra in a distorted square antiprism.

MgH_2

- *Classic* metal hydride
- High capacity (≈7.6 wt.%)
- High temperature hydride

Mg structure

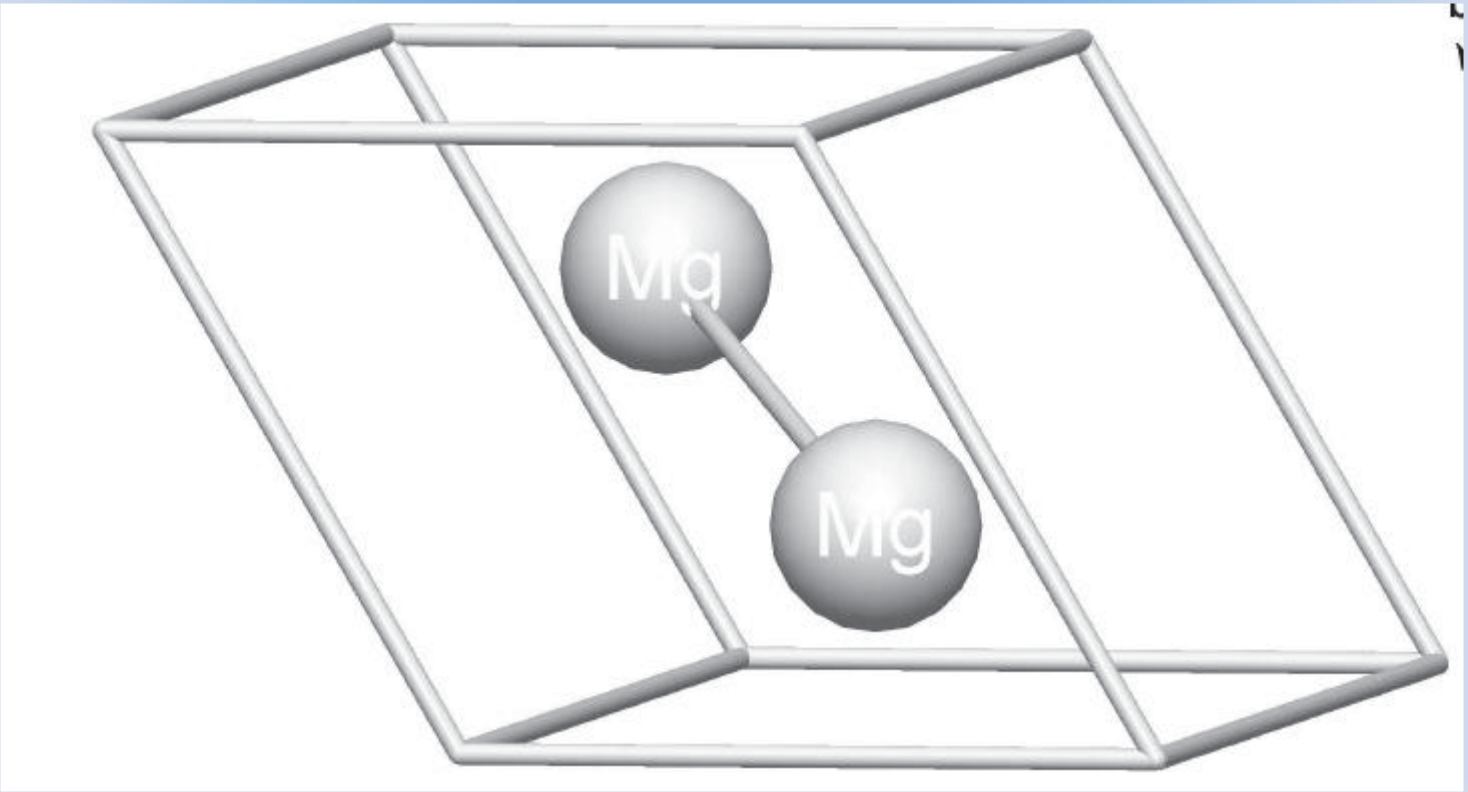

hP2, P6_3/mmc

UQTR
Université du Québec
à Trois-Rivières

MgH_2 structure

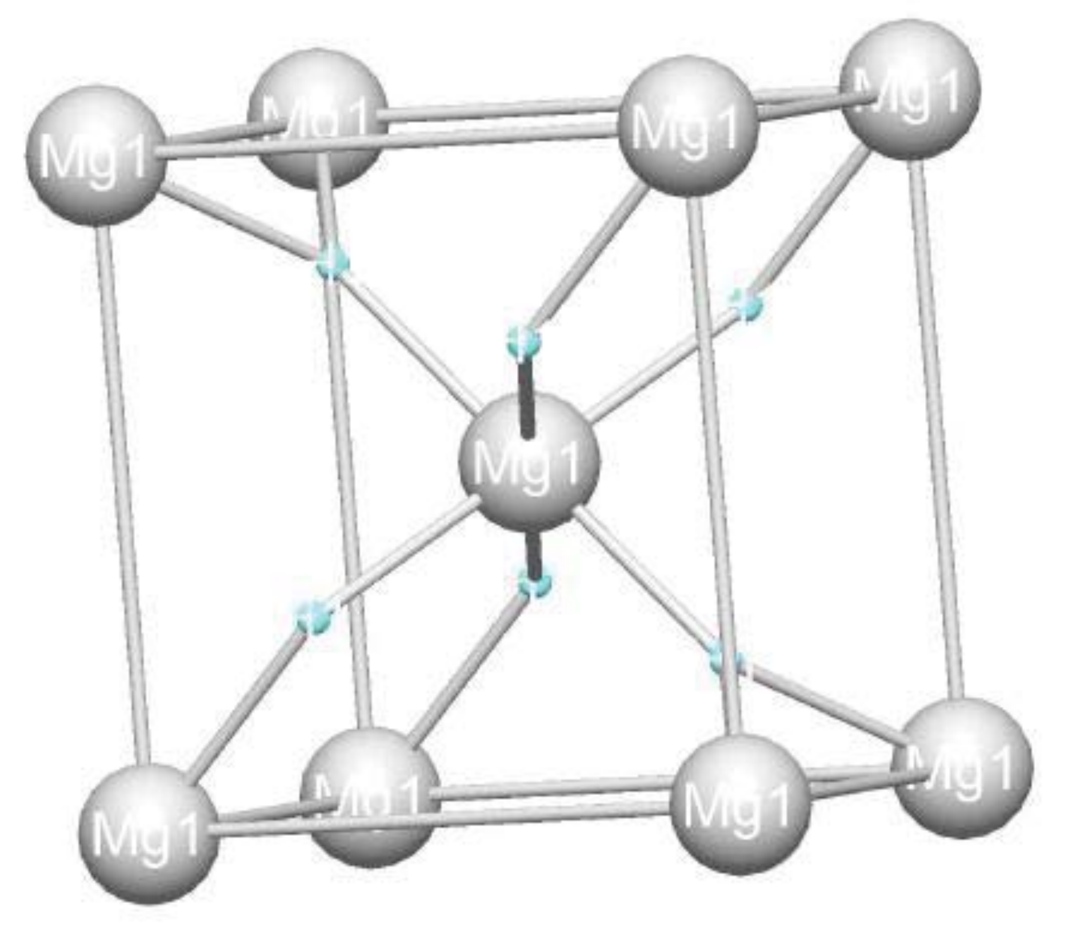

tP6, $P4_2/mnm$

UQTR
Université du Québec
à Trois-Rivières

Mg X-ray pattern

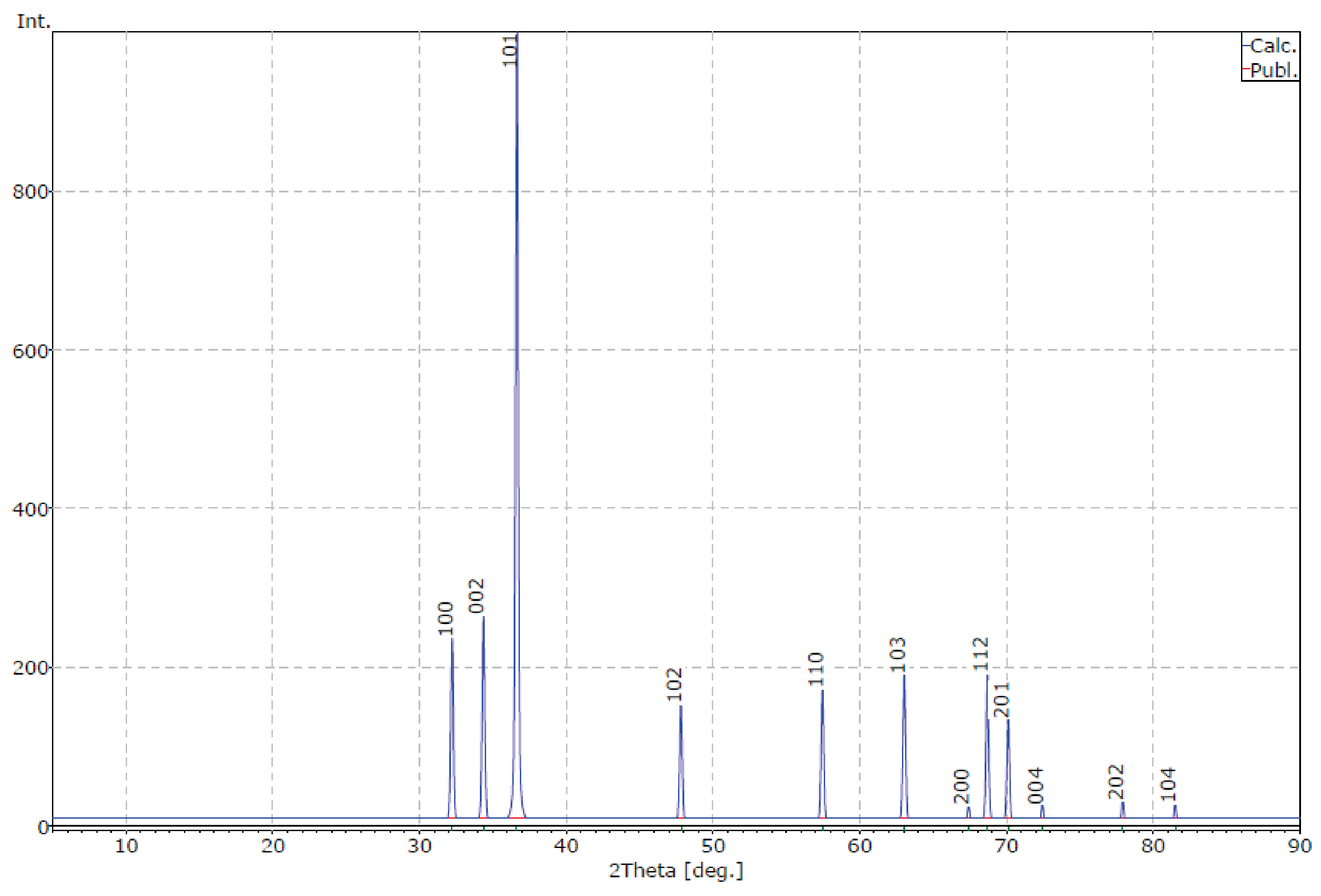

Université du Québec
à Trois-Rivières

MgH_2 X-ray pattern

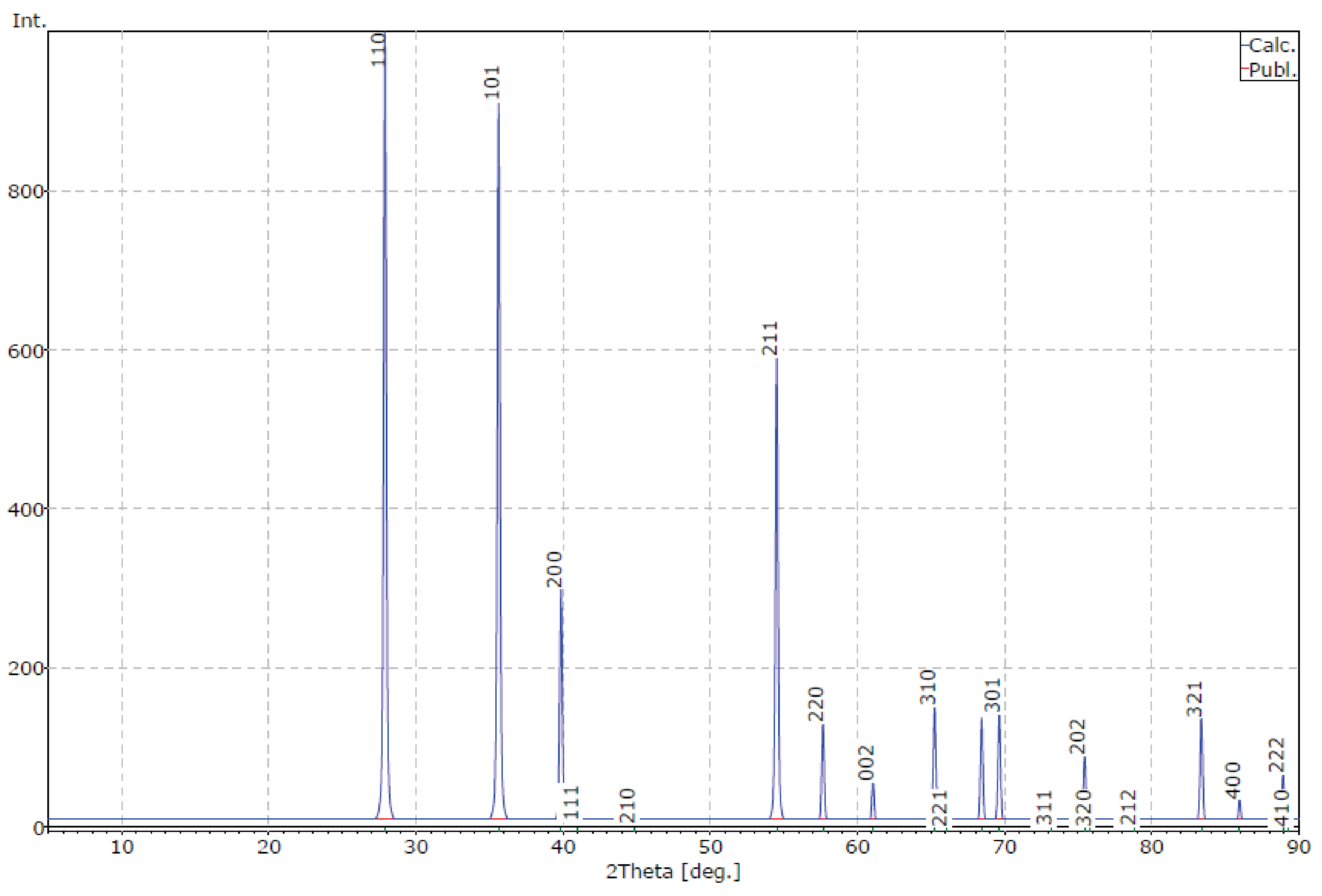

Université du Québec
à Trois-Rivières